SIMULATING THE EFFECT OF WATER ON THE FRACTURE SYSTEM OF SHALE GAS WELLS

A Thesis

by

HASSAN HASAN H. HAMAM

Submitted to the Office of Graduate Studies of
Texas A&M University
in partial fulfillment of the requirements for the degree of

MASTER OF SCIENCE

August 2010

Major Subject: Petroleum Engineering

SIMULATING THE EFFECT OF WATER ON THE FRACTURE SYSTEM OF SHALE GAS WELLS

A Thesis

by

HASSAN HASAN H. HAMAM

Submitted to the Office of Graduate Studies of
Texas A&M University
in partial fulfillment of the requirements for the degree of

MASTER OF SCIENCE

Approved by:

Chair of Committee,	Robert A. Wattenbarger
Committee Members,	J. Bryan Maggard
	Wayne M. Ahr
Head of Department,	Stephen Holditch

August 2010

Major Subject: Petroleum Engineering

ABSTRACT

Simulating the Effect of Water on the Fracture System of Shale Gas Wells.

(August 2010)

Hassan Hasan H. Hamam, B.S., West Virginia University

Chair of Advisory Committee: Dr. Robert A. Wattenbarger

It was observed that many hydraulically fractured horizontal shale gas wells exhibit transient linear flow behavior. A half-slope on a type curve represents this transient linear flow behavior. Shale gas wells show a significant skin effect which is uncommon in tight gas wells and masks early time linear behavior. Usually 70-85% of frac water is lost in the formation after the hydraulic fracturing job. In this research, a shale gas well was studied and simulated post hydraulic fracturing was modeled to relate the effect of frac water to the early significant skin effect observed in shale gas wells.

The hydraulically fractured horizontal shale gas well was described in this work by a linear dual porosity model. The reservoir in this study consisted of a bounded rectangular reservoir with slab matrix blocks draining into neighboring hydraulic fractures and then the hydraulic fractures feed into the horizontal well that fully penetrates the entire rectangular reservoir.

Numerical and analytical solutions were acquired before building a 3D 19x19x10 simulation model to verify accuracy. Many tests were conducted on the 3D model to match field water production since initial gas production was matching the analytical

solutions before building the 3D simulation model. While some of the scenarios tested were artificial, they were conducted in order to reach a better conceptual understanding of the field.

Increasing the water saturation in the formation resulted in increasing water production while lowering gas production. Adding a fractured bottom water layer that leaked into the hydraulic fracture allowed the model to have a good match of water and gas production rates. Modeling trapped frac water around the fracture produced approximately the same amount of water produced by field data, but the gas production was lower. Totally surrounding the fracture with frac water blocked all gas production until some of the water was produced and gas was able to pass through. Finally, trapped frac water around the fracture as combined with bottom water showed the best results match.

It was shown that frac water could invade the formation surrounding the hydraulic fracture and could cause formation damage by blocking gas flow. It was also demonstrated that frac water could partially block off gas flow from the reservoir to the wellbore and thus lower the efficiency of the hydraulic fracturing job. It was also demonstrated that frac water affects the square root of time plot. It was proven by simulation that the huge skin at early time could be caused by frac water that invades and gets trapped near the hydraulic fractures due to capillary pressure.

DEDICATION

I dedicate this work to the Almighty God, for all the blessings, strength, protection, and guidance HE grants me every single day of my life. I also dedicate this work to my caring family members and my all time encouraging friends who have lovingly supported me throughout my life and made my work complete.

ACKNOWLEDGEMENTS

The author of this thesis wishes to express his deep gratitude and appreciation to the following people who provided me with guidance, support, and advice in every step of my work and contributed greatly to this study. I would like to thank my advisor, Dr. Robert. A. Wattenbarger, for being a mentor, advisor, and a friend to me. His guidance, dedication, sincerity, and support guided me to the completion of this work. I am very honored to have worked with him and I am grateful to him for giving me this opportunity to work with him. I would also like to thank Dr. Bryan Maggard and Dr. Wayne M. Ahr for their active contribution.

I would like to thank Tai Pham, EOG Resources, for providing the data to be studied and analyzed which made this study much easier.

I would like to thank Saudi Aramco for giving me the opportunity to come to Texas A&M for my masters in petroleum engineering under their supportive scholarship program.

I would like to acknowledge the never ending support of my parents, Hasan and Fawzeyah, my wife Roaa, and my son Abdulelah.

I want to thank all my professors, friends, and colleagues who supported and helped me the best they could, and made my life and work enjoyable.

TABLE OF CONTENTS

LIST OF TABLES

LIST OF FIGURES

FIGURE Page

FIGURE Page

CHAPTER I

INTRODUCTION

The Barnett Shale is one of the largest onshore natural gas fields in North America, and the biggest in the state of Texas. Over the past decade, shale gas has become a very valuable source of natural gas in the United States and other parts of the world. Some studies forecast that shale gas will be responsible for providing 50% of the natural gas production in North America by 2020.

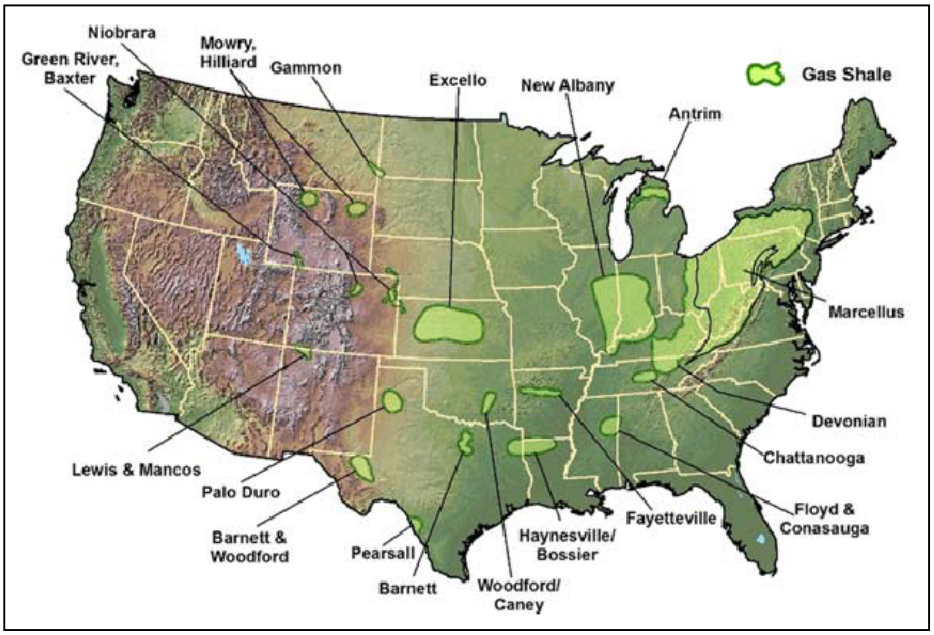

Fig. 1.1 - Shale gas plays in the United States (Arthur et al. 2009)

This thesis follows the style of *Society of Petroleum Engineers Journal*.

The boundaries and the size of the Barnett Shale has been estimated many years ago, but due to the very low permeability of the formation, not many attempts were made to recover the entrapped gas. The Barnett Shale is considered to be a "tight" gas reservoir. In order to produce these formations in commercial quantities, hydraulic fracturing is required to stimulate the very low formation permeability. Higher gas prices, advanced technology in horizontal wells, and hydraulic fracturing have played a major role in making shale gas producible in commercial quantities and production of gas that was considered unrecoverable.

Fig. 1.1 shows a map of the different shale gas plays in the united states that were approximated in 2009.

Transient linear flow behavior is observed in shale gas wells. This behavior is characterized by a half-slope on the log-log plot of the gas production rate versus time plot, or by a straight line on the $\left[m(p_i)-m(p_{wf})\right]/q_g$ *vs.* $\sqrt{t}$ plot (square root of time plot).

It was noticed that many shale gas wells show a huge early “skin effect”. The skin effect influences early time linear behavior. Many attempts have been made to discover the reason for this skin including the possibility of well damage, but none were successful at modeling this significant skin indicated by the significant y-intercept. Fig. 1.2 shows an example of the linear transient behavior with the huge skin at early time. The skin is indicated by the skewed data at early time. A well not exhibiting a huge early time skin would go through the origin on the square root of time plot.

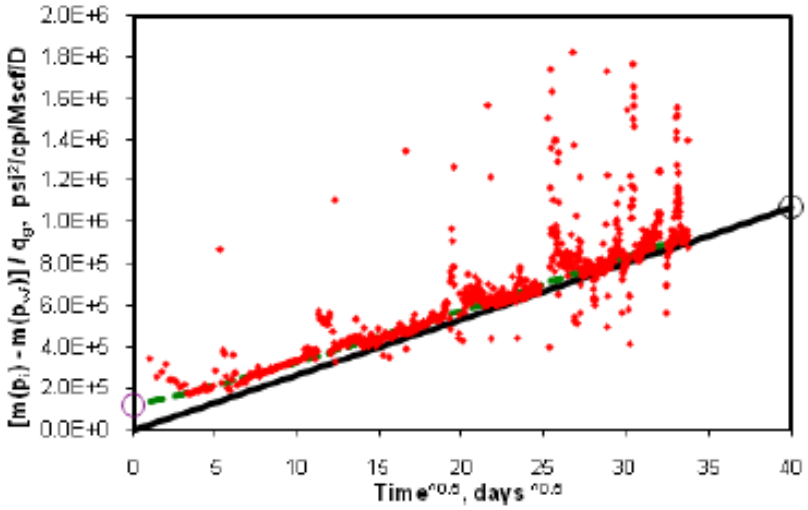

Fig. 1.2 - Square root of time plot of shale gas well showing a high skin effect at early time

1.1. Gas and Water Diffusivity

Early studies regarding shale gas ignored the effect of water and considered it insignificant. There were a few reasons behind ignoring the effect of water besides simplifying the studies. The main reason water was ignored is because shale gas wells are dominated by gas. Looking at the diffusivity equation, it can be clearly seen that mobility and compressibility are dominated by gas. Eqn. 1 shows the water diffusivity equation. Eqn. 2 shows the gas diffusivity equation. Eqn. 3 shows the dimensionless time equation.

$$\nabla^2 p = 0.00633 \frac{\phi \mu c_t}{k} \frac{\partial p}{\partial t} \quad \text{.....} \quad (1.1)$$

$$m_D = \frac{kh\left[m(p_i) - m(p_{wf})\right]}{1422 q_g T} \quad \text{.....} \quad (1.2)$$

$$t_D = \frac{kt}{\phi \mu c_t A_c} \quad \text{.....} \quad (1.3)$$

Fig. 1.2 shows the square root of time plot of an example well with the significant skin effect at the early time intercept.

In this research, we will study the effect of water on the fracture system and confirm or disprove that frac water as a possible reason behind very large skin effect at early time on shale gas wells.

1.2. Problem Description

Barnett Shale is a tight gas formation. In order to produce gas from this hard shale, the formation has to be hydraulically fractured.

In Barnett Shale, hydraulic fracturing is done by pumping water into the wellbore at a certain pressure to create and propagate a fracture in the surrounding formation downhole. This process allows for more surface area to be exposed and therefore large quantities of gas to be produced.

Shale gas reservoirs behave as if they are controlled by transient linear flow. This behavior is characterized by a half-slope on the log-log plot of gas rate versus time or a straight line of the $\left[m(p_i) - m(p_{wf})\right] / q_g$ *vs.* $\sqrt{t}$ plot (square root of time plot). Shale gas wells usually show a very large "skin effect". The skin effect influences the early time linear behavior. Many theories were delivered to explain the reason for this skin including the possibility of well damage, but none were successful at explaining the large skin observed at early time.

The only way to produce the very tight compressed shale is through hydraulic fracturing. The process of hydraulic fracturing includes pumping water, sand, and additives into the wellbore and down the casing under extremely high pressure. As the mixture is forced out through the perforations and into the surrounding rocks, the pressure causes the shale to fracture. This process creates fairways connecting the reservoir to the well and allows the reservoir gas to flow to the wellbore. Most of the injected fracturing fluid is lost in the formation and is not recovered using the cleanup process before producing the well.

In this paper, we will study the effect of pumped frac water as well as some other sources of water on the fracture system and confirm or disprove that frac water is a possible reason behind very large skin effect at early time on shale gas wells.

1.3. Shale Gas Geology

Shale is a sedimentary rock that is composed of consolidated clay-sized particles. Shale gas is a natural gas produced from tight shale formations. Shale gas mainly consists of methane, and is usually a dry gas. Looking at the depositional environment of shale gas, shales are deposited as muds in low-energy environments such as lakes, seas, inland oceans and similar environments where fine-grained clay particles fall out of suspension in the quite waters. The fine grains and laminated layers of sediments are the main reasons shale gas has low horizontal permeability and very low vertical permeability **(Arthur et al. 2009).**

The Fort Worth basin is a shallow, north-south-elongated trough in north-central Texas. Fig. 1.3 shows a generalized stratigraphy of the basin. The basin was formed

during the Paleozoic era (mainly Mississippian and Pennsylvanian). **Montgomery et al. 2005** divided the total Paleozoic section into three intervals depending on their tectonic history:

1. Cambrian-Upper Ordovician strata (Riley-Wilberns, Ellenburger, Viola, Simpson)
2. Middle-Upper Mississippian strata (Chappel, Barnett Shale, Lower Marble Falls)
3. Pennsylvanian-strata (Upper Marble Falls Formation, Atoka, etc.).

The top of the Ellenburger is an erosional surface characterized by solution-collapse features. Overlying Upper Ordovician Viola and Simpson rocks are confined to the northeastern part of the basin. The zero edge of the Viola–Simpson is a crucial stratigraphic boundary because south and west of it, Mississippian rocks rest directly upon karsted, potentially water-bearing Ellenburger carbonates. **Montgomery et al. 2005.**

To the east, the lower Barnett lies directly above a regional angular unconformity, while In the core central area it rests on the Ordovician Viola Limestone or slightly older Simpson Group. To the West, the lower Barnett rests on the Ordovician Ellenburger Group. The Forestburg limestone separates the lower and upper Barnett shale members. The Forestburg thins rapidly to the south across the Barnett productive area as shown in Fig. 1.3.

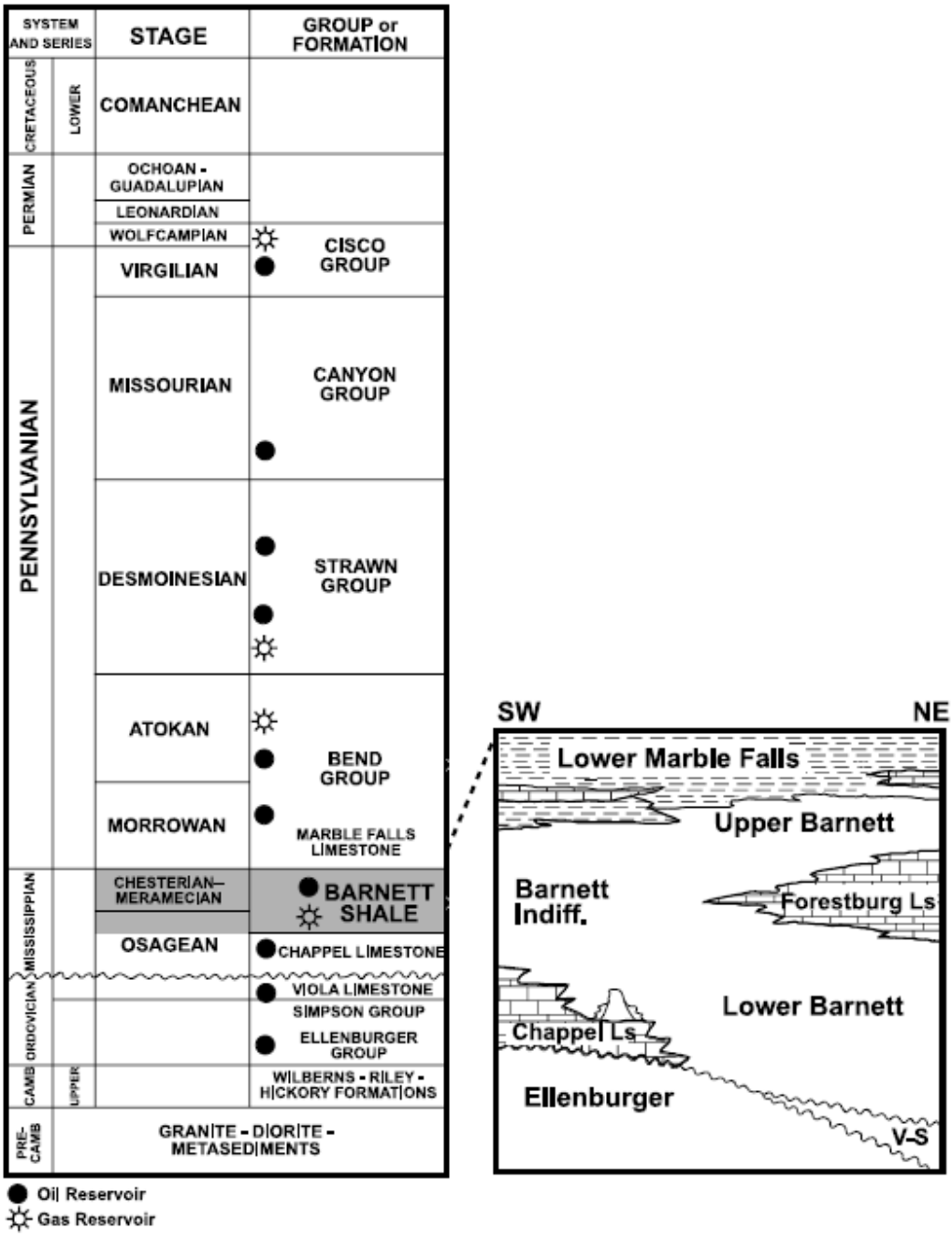

Fig. 1.3 - Fort Worth generalized stratigraphy and the Viola Simpson western limits

The Fort Worth basin has potential for great gas production, but several factors need to be taken into consideration before such development such as the Erosional pinch-out of the Viola-Simpson. The V-S formation acts as a lower barrier to hydraulic fracture growth and places lower Barnett Shale on the potentially water-bearing Ellenburger Group and thus creating potential water incursion after stimulation. **Montgomery et al. 2005.** Fig 1.4 shows a map of the Barnett shale producers in the state of Texas and the western boundary of the Viola Simpson limits.

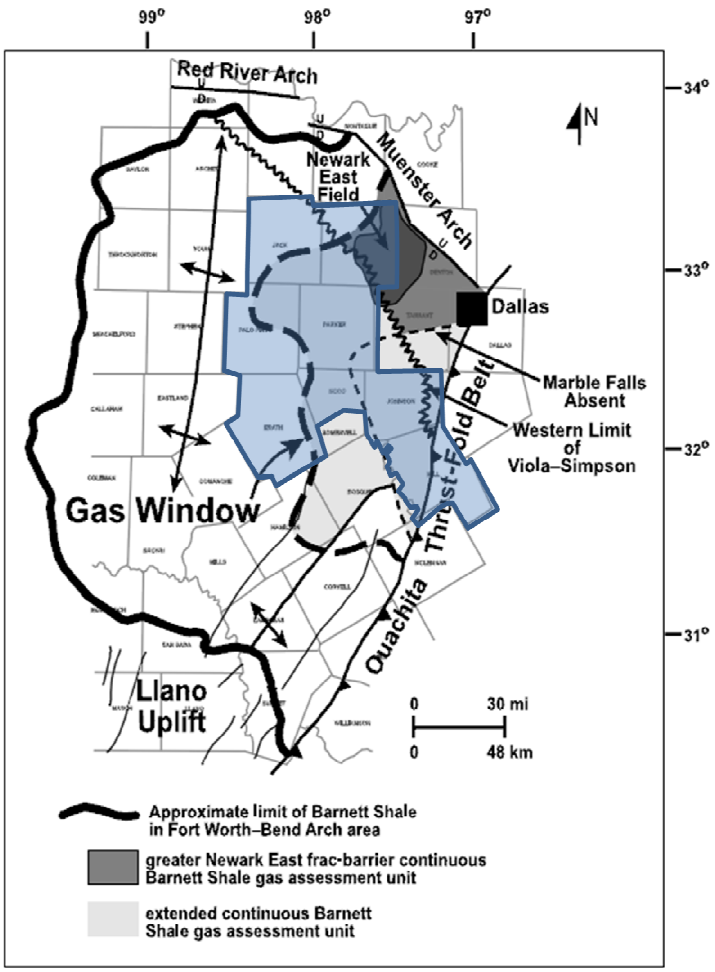

Fig. 1.4 - Barnett Shale producers in Texas and the western limits of the Viola Simpson

1.4. Objectives

The objectives of this research are

- Study the production data for shale gas wells.
- Select a Shale Gas well with complete production data to be a case study.
- Generate a semi-analytical solution model using the Stehfest Algorithm program.
- Use GASSIM (2D Gas and Water Simulator) to verify the Stehfest solution.
- Use a 3D Commercial Simulator (CMG) to further verify the previous solutions with gas only flowing.
- Using CMG, introduce water in the fractures and match the model with the available gas production data.
- Match the water production using CMG with the actual field data.
- Run various scenarios for water production.
- Study the effect of water on the gas production.
- Observe any difference in gas production behavior while modeling various water production scenarios.
- Study the fracture spacing and the efficiency of the fracture job and determine optimal fracture spacing if possible.

1.5. Organization of this Thesis

The study is divided into six chapters. The outline and organization of this thesis are as follows:

Chapter I presents an overview of the shale gas. The research problem is described and the objectives are stated.

Chapter II presents the previous work and literature in this area of study. Linear flow analysis, dual porosity linear flow, early skin effect, and early skin effect period are also reviewed.

Chapter III describes the theoretical analysis and the theory behind the model to be used in this research. The chapter also details how the full well model was scaled down to the model simulated here.

Chapter IV presents analytical and reservoir simulation modeling. Model verification and step by step simulation are also presented.

Chapter V explains the different simulation cases and scenarios and then summarizes their results. Analysis of the results and findings are also shown.

Chapter VI presents the conclusions and recommendations of this thesis.

CHAPTER II

LITERATURE REVIEW

2.1. Introduction

Early literature regarding shale formations ignored the effect of water. The reason behind that is because in shale gas wells, mobility and compressibility are dominated by gas. This chapter will summarize previous related work on linear flow analysis, dual porosity linear flow analysis, hydraulic fracturing techniques, early skin effect period, and shale gas frac fluids.

2.2. Linear Flow Analysis

Shale gas wells behave as if they are controlled by transient linear flow. This behavior is represented by a half-slope on the log-log plot of gas rate versus time or a straight line on the $\left[m(p_i) - m(p_{wf})\right]/q_g$ *vs.* $\sqrt{t}$ plot (also known as Square Root of Time). **(Al-Ahmadi et al. 2010)**.

Early literature studies showed different methods for shale gas well analysis. Type-curves for single and dual-porosity shale gas reservoirs were presented by **Lewis and Hughes (2008)** using an adjusted material balance time. **Medeiros et al. (2008)** presented a semi-analytical solution for horizontal well with multiple traverse fractures. A summary of methods used for shale gas analysis was presented by **Mattar et al. (2008)**. **Wattenbarger (2007)** showed different causes for linear transient flow.

Different analysis of linear flow in gas well production were presented by **El-Banbi (1998).**

2.3. Dual Porosity Linear Flow Analysis

Naturally fractured shale gas reservoirs were described by dual porosity model which was initially made by **Barenblatt et al. (1960)**. Warren and Root created the foundations of today's analysis of naturally fractured reservoir **(Warren and Root 1962)**. They modeled naturally fractured reservoirs by a uniform homogenous matrix blocks separated by fractures where matrix blocks supply fluid and the fractures move them as shown in Fig. 2.1.

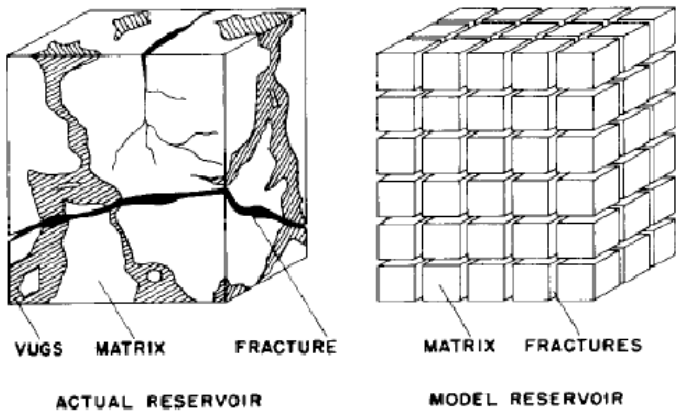

Fig. 2.1 - Warren & Root Dual Porosity Model (Warren & Root 1962)

The assumptions made in this study are similar to the ones that were made by **Al-Ahmadi et al. (2010)**. The shale gas well in this study is idealized as producing from a rectangular dual porosity reservoir where the flow moves from matrix blocks into a system of hydraulic fractures. It is assumed that there is no flow outside the fracture

system. Therefore, the shale gas well system is a linear dual porosity one, and the solutions were presented in earlier study by **El-Banbi (1998)** as Laplace domain solutions.

Two distinct theoretical models were presented by **Al-Ahmadi et al. (2010)** that described linear flow in dual porosity systems, Fig. 2.2. Only Model 1 will be used in this research while Model 2 will be ignored. Model 1 as described by **Al-Ahmadi et al. (2010)** as a linear dual porosity "transient slab model". The hydraulic fracture system in the model originates from the perforation clusters in the wellbore. The perforation clusters were assumed to be equally spaced. The matrix formation was assumed to be homogeneous regardless if it contains natural fractures or not.

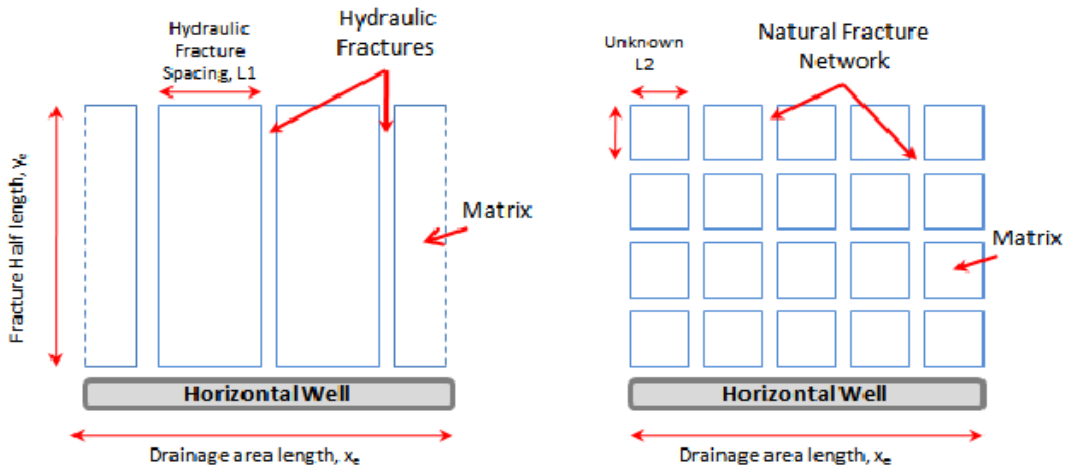

Fig. 2.2 - Model 1 and model 2 as described by Al-Ahmadi (Al-Ahmadi et al. 2010)

El-Banbi (1998) introduced solutions for the transient dual porosity linear reservoir model. **Bello (2009)** identified five flow regions that described a horizontal well's life production based on El-Banbi's solutions. Fig. 2.3 shows an example of

Bello's five flow regions in a horizontal well. Bello found the transient drainage from the matrix blocks to the fracture system which he described as Region 4, is the dominant flow regime in the early years for the majority of shale gas wells.

(Bello & Wattenbarger 2008, 2010) introduced an equation that described the flow for Region 4. The equation for linear transient flow from matrix blocks can be written as:

$$\frac{\left[m(p_i)-m(p_{wf})\right]}{q_g}=\tilde{m}_4\sqrt{t} \qquad \text{.....} \qquad (4)$$

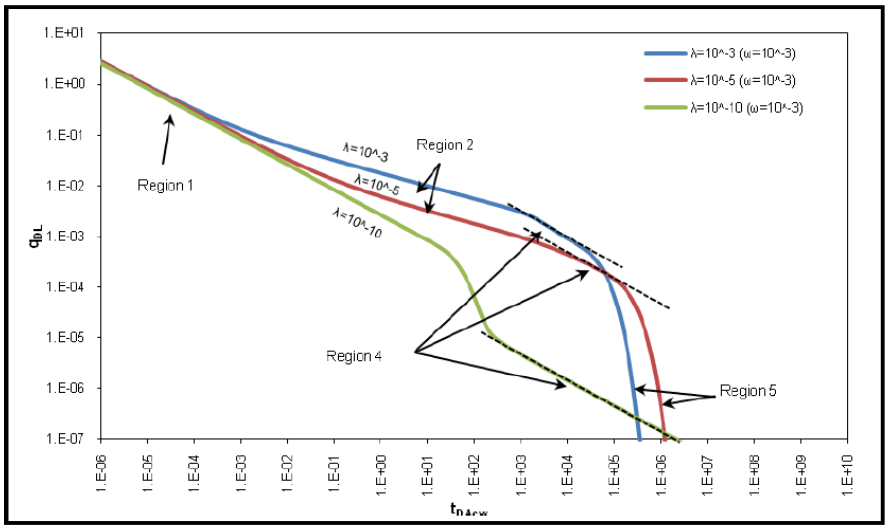

Fig. 2.3 - Bello's five flow regions in horizontal wells (Al-Ahmadi et al. 2010)

2.4. Early "Skin Effect" Period

Using Model 1, **Al-Ahmadi et al. (2010)** found out that most shale gas wells show a large intercept on the $\left[m(p_i)-m(p_{wf})\right]/q_g$ *vs.* $\sqrt{t}$ plot. There were a few theories

regarding this early "skin effect" such as the well cleanup of water from the hydraulic fracturing treatment, but nothing was tested. Bello **(Bello 2009; Bello & Wattenbarger 2009, 2010)** considered this early skin effect as a constant skin.

Wang et al. (2009) categorized fracture damage as either damage inside fracture, or damage inside the formation. Proppant crushing, proppant embedment, fracture face damage, or fracture plugging with chemicals and polymers could cause damage inside fractures. Damage inside the reservoir could be caused by excessive fluid leakoff, clay swelling, relative permeability changes, or capillary effects.

2.5. Shale Gas Frac Water

One of the biggest problems regarding completing shale wells is the recovery of injected fluids. It is not uncommon to leave 90% of injected fluid in the formation while recovering only 10% and that result in lower the relative permeability to gas. In the Barnett Shale, frac water is generally pumped at high rates. 100 BPM is a common number when stimulating long horizontal areas such as the Barnett Shale **(Palisch et al. 2008)**.

Holditch (1979) investigated different factors affecting water blocking in hydraulic fractured gas wells and found that reservoir properties such as capillary pressure, capillary hysteresis, and relative permeability are extremely imporntat in determining the cleanup behavior.

CHAPTER III

THEORETICAL ANALYSIS

3.1. Segmented Model and Theory

A few assumptions were made while conducting this research and they were the key concepts in building the basic and complex models.

1) Hydraulic fractures are caused by perforation clusters to the wellbore.
2) The hydraulic fracture spacing is fixed and is the same throughout the well.
3) We are simulating one half the distance between two hydraulic fractures. The entire well consists of 112 segments. We are assuming that all of them are identical.
4) Each segment is bounded by a hydraulic fracture from one side, a no flow boundary from another side, a horizontal well, and the top and bottom of the reservoir.
5) The fluid, pressure, and overall well behavior at any hydraulic fracture is the assumed to be the same at any other hydraulic fracture throughout the well.
6) Frac water that is left in the formation has the same properties and behaves the same as regular water.

The theory behind this study is simple and is focused on the effect of water on the fracture system. The model is not going to be used for complicated long term forecasting. For that reason, a small segmented model was created and idealized throughout the entire well. The model has to be accurate first so its results would be

reliable. Before jumping to simulation, the model will first be replicated using different types of distinct solution approaches to verify accuracy and consistency.

Fig. 3.1 shows the entire proposed well model in this research. It consists of a horizontal well cutting through the matrix formation. The matrix formation is divided by equally spaced hydraulic fractures.

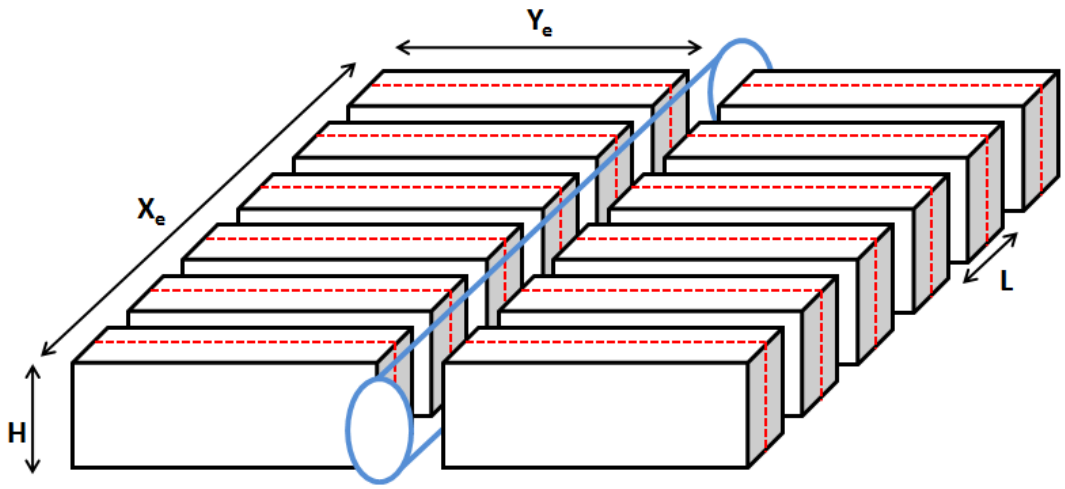

Fig. 3.1 - Schematic of slab matrix linear model of hydraulically fractured well

Shale gas wells produce through hydraulic fractures. The first flow that happens is through the hydraulic fractures since they act as pathway that connects the reservoir to the wellbore. When producing the shale gas, pressure in the fractures drops very rapidly which forces the surrounding fluid in the matrix formation to rush to the fracture. The initial pressure drop in the fracture system is a very fast process which usually happens within a few hours or even minutes.

3.2. Well Model to Segment Model

The conversion between the proposed entire well model scenario to a segment model was made for many reasons. The main reason is that, we are assuming fixed fracture spacing and other parameters throughout the well which makes the segmented model the perfect candidate to capture little details which could be ignored in a full model with a much finer grid blocks.

Fig. 3.2 shows a full matrix formation slab and its conversion to the segment slab model. The same concepts that were applied for the entire well is applied on the segmented model which depends on the rapid pressure drop across the fracture face. The segment model produces gas through the hydraulic fracture face only and the model is bounded by half a hydraulic fracture from one side, a no-flow-boundary, and the top and bottom of the reservoir.

Fig. 3.3 is an illustration showing the hydraulic fractures, the no-flow-boundaries, and the segmented model part.

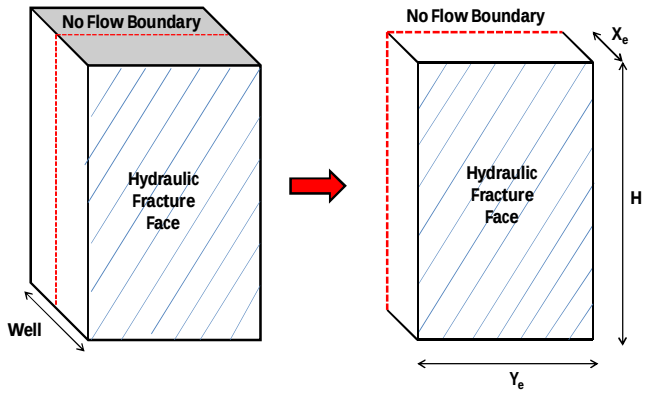

Fig. 3.2 - Single matrix slab conversion to segmented model

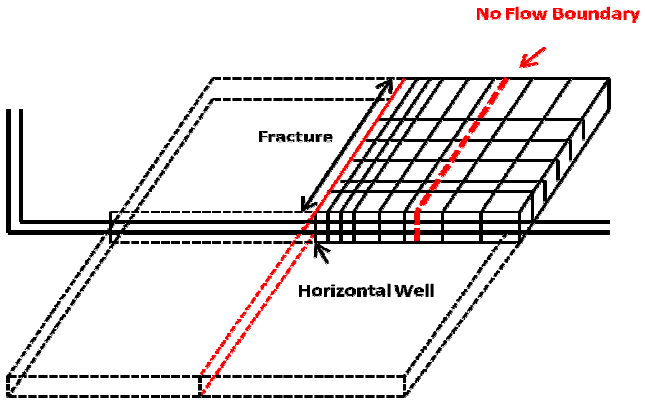

Fig. 3.3 - General illustration showing the segmented model

The simulation model in this study represents half the distance between two fractures (assuming the fracture spacing is constant). It was expected to either fully simulate the whole fracture or simulate half of the fracture to be part of the model. In this research, we chose to simulate the full fracture width since it is very small to begin with. In order to have an accurate model, a data trick was used to compensate for using the full fracture width. Eqn. 3.3 and Eqn. 3.4 shows the equations used to represent the fracture permeability and porosity using the data tricks.

$$F_{CD} = \frac{k_f w}{k x_f} = \frac{k_{inside} w}{k_m x_f} \quad \text{..... (3.1)}$$

$$k_f = k_{inside} \frac{\omega}{L} \quad \text{..... (3.2)}$$

$$k_f = \frac{k_{inside}}{2} \quad \text{..... (3.3)}$$

$$\phi_f = \frac{\phi}{2} \quad \text{..... (3.4)}$$

CHAPTER IV

ANALYTICAL AND MODEL BUILDING

4.1. Model Verification

In order to run complex cases and different scenarios with confidence that the results are reliable, a simple case was run using different solution models. The testing case was a basic single phase gas with connate water. Since it is a simple single phase case, we are expecting the results to be approximately the same using different solutions. Matching the single phase case using different methods provide a verification process in order to verify validity of two phase cases in 2D and 3D.

Well # 314 was used as a case study in this research for building the analytical and simulation model. The well was a good candidate for this research because it exhibits the early time skin and it has complete production data. Table 4.1 shows a summary of the reservoir and completion data for Well # 314, while Fig. 4.1 shows the production data of the same well.

Table 4.1 - Well # 314 Data

Porosity, ϕ(fraction)	0.06	**B_{gi} (rcf/scf)**	0.00509
Viscosity, μ_{gi}(cp)	0.0201	**$m(p_i)$ (psi^2/cp)**	5.97×10^{8}
Total Compressibility, c_{ti}(psi^{-1})	220×10^{-6}	**$m(p_w)$ (psi^2/cp)**	2.03×10^{7}
Gas Saturation, S_{gi}	0.7	**Number of Perforation Clusters, n_f**	28
Reservoir Temperature, T(^oR)	610	**Reservoir Thickness, h(ft)**	300
Matrix Permeability, k_m(md)	1.5×10^{-4}	**Drainage Area (Well) Length, x_e(ft)**	2968
Acw	1780800	**Y_{De} (ft)**	173.5
Lambda (λ)	0.285283019	**Gas Gravity**	0.65
Omega (ω)	0.001	**L (ft)**	106
Pwf (psi)	500	**Initial Reservoir Pressure (psi)**	2950
Skin (Elbanbi)	9.79	**Model**	Transient-Slab

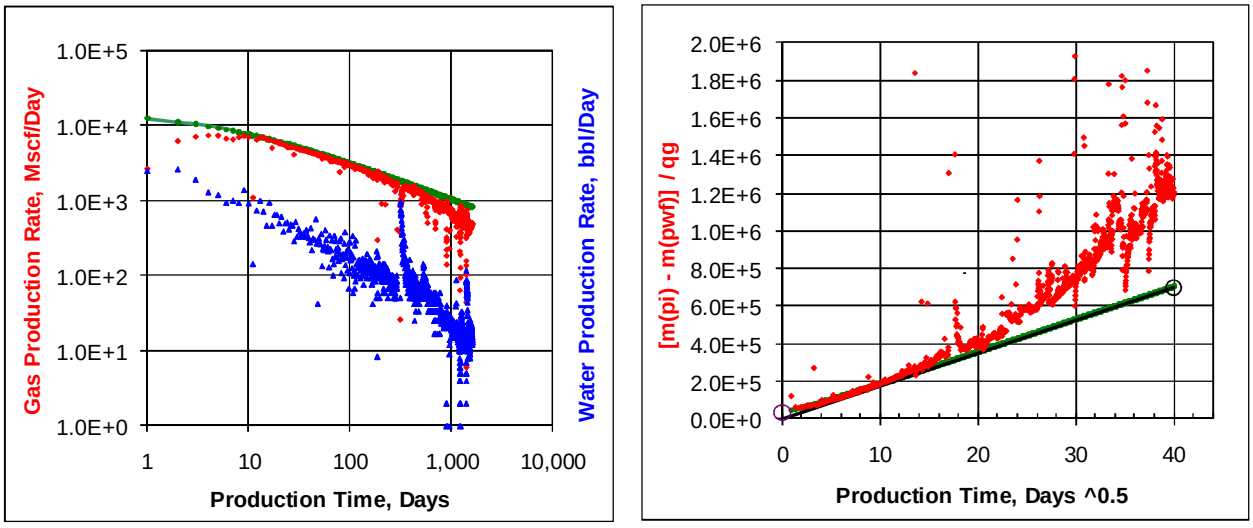

Fig. 4.1 - Gas and water production rates vs. time (on left). The square root of time plot (on right) shows the early time skin as well as the end of transient flow as the boundary is reached after 225 days.

4.2. Simulation Steps

Step 1: Simulation of Single-Phase Flow Using Stehfest Semi-Analytical Solution Model

The first step in modeling post-fracture treatment behavior was to simulate the ideal, single-phase flow case. The first case was run using the Stehfest Algorithm **(Stehfest 1970)** assuming 100% gas-saturation. The Stehfest solution is a Semi-Analytical solution in the dimensionless Laplace space. These solutions were converted to real time in order to compare them with the other solutions and results. Since the Stehfest algorithm assumes constant gas properties throughout the life of the well (neglects increasing gas compressibility during depletion), it is expected that gas production rate plot declines faster than any other methods for boundary dominated

flow. Fig. 4.2 shows the Stehfest solution compared to the field data on the square root of time plot. The results from this method would still be reliable for the early time until the boundary dominated flow develops.

A 1 Dimensional case was run and solutions were generated using Stehfest Algorithm. The next steps will be simulating the same case, but with a few changes. A program developed in house using Stehfest Algorithm was used to generate a semi-analytical solution. Data and parameters from table 1 were used in building up the Stehfest solution model.

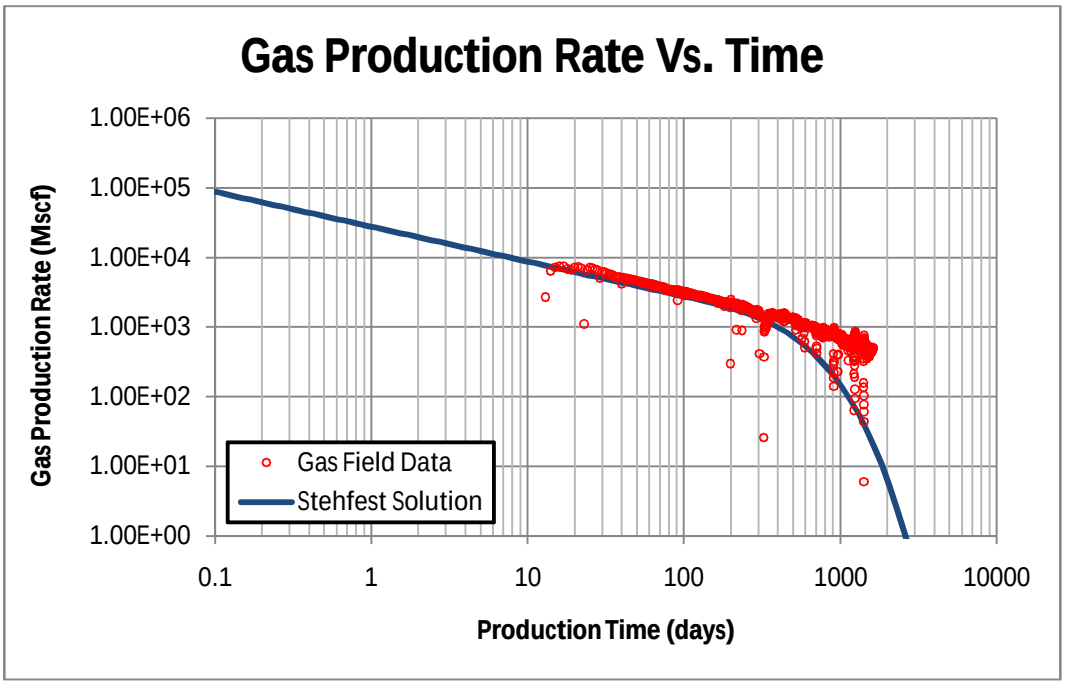

Fig. 4.2 - Gas production rates vs. time using Stehfest algorithm

Step 2: Simulation of Single-Phase Flow using a 2 Dimensional Gas Simulator (GASSIM)

After generating a semi-analytical solution for the study case, a more complex scenario was developed. The second method that was used in this study was a two phase Simulator called GASSIM. The exact case was run but a 30% water saturation was added. The model that was built was 19x19x1. The first cell of the x-direction represented the hydraulic fracture, while the first cell of the y-direction represented the horizontal well. The horizontal well produced only from the hydraulic fracture.

This model has very fine grids near the wellbore and fracture, but became more coarse as we went away towards the no flow boundary. Doing that would help us to observe the fluid behavior around the wellbore very precisely. It is important to note that the model that was built simulates one segment, so, the acquired results were multiplied by 112 to account for the entire well.

The results that were obtained from this run were plotted against the ones from that were acquired from Stehfest solutions on a square root of time plot as shown in Fig. 4.3.

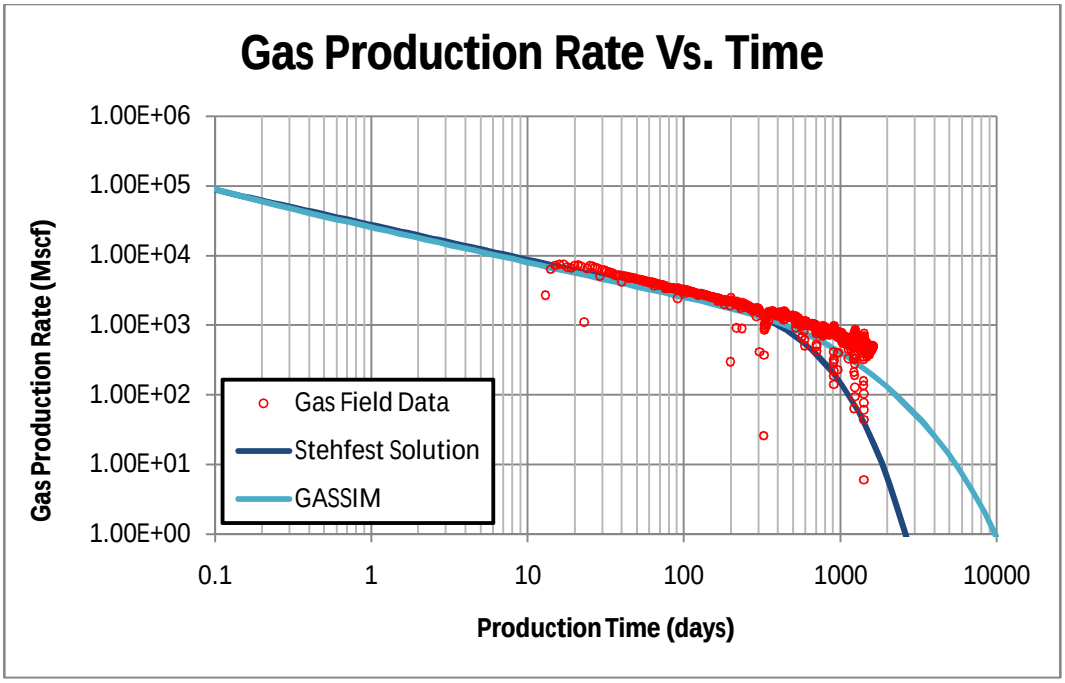

Fig. 4.3 - Gas production rates vs. time using Stehfest algorithm and GASSIM. Note that Stehfest curve underestimates the gas production at boundary dominated flow

Step 3: Simulation of Single-Phase Flow using (CMG)

The next step was to simulate the exact same case as in step 2 but with a commercial simulator that is capable of running complex cases. The 3rd case was run using a commercial simulator (CMG) and the test case was again the same 2D case, with gas only flowing and 30% connate water saturation. This case is identical to the GASSIM case in using the same grid, fracture, and overall properties. The constructed simulation model was 19x19x1. The simulation model represented the hydraulic fracture by a thin column that had the properties of the hydraulic fracture. The well in this case was draining from the hydraulic fracture only. The gas production using CMG matched the results which was obtained earlier from GASSIM and from Stehfest Algorithm.

Step 4: Simulation of Gas/Water Two-Phase flow in 2D using CMG

This step shows the first step in converting the model to a two-phase model. The hydrauilc fractures were totally filled with water, while rest of the parameters were the same. Fig. 4.4 shows a comparison between the single-phase model with the two-phase model.

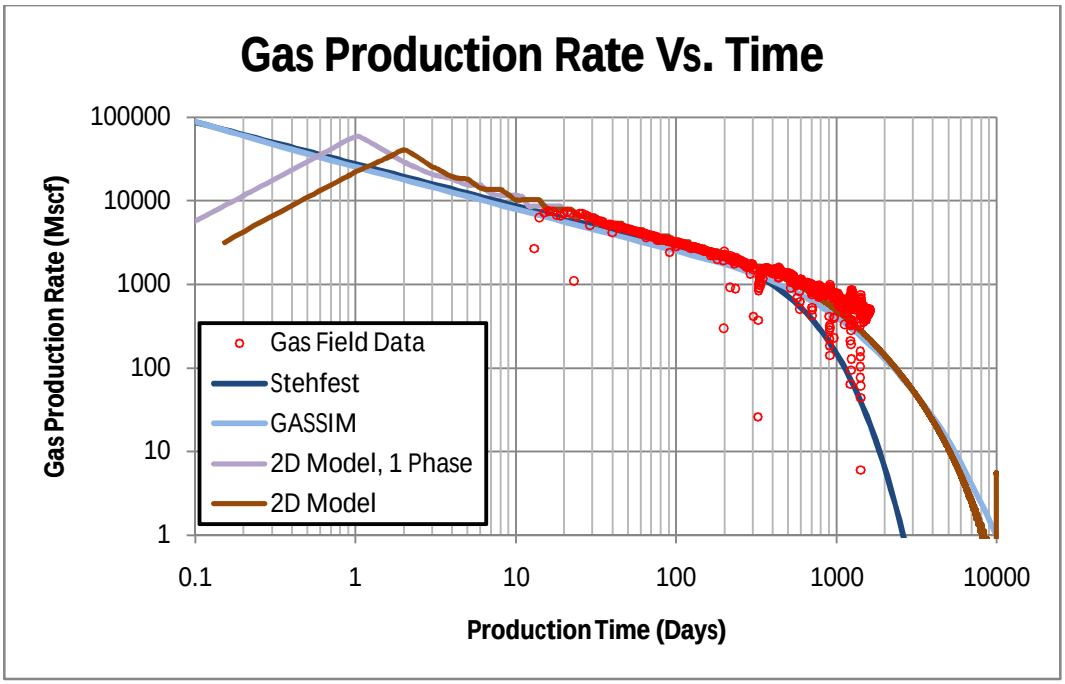

Fig. 4.4 - 2D model verification, the plot shows the 2D single phase model as well as the 2D two phase model and their results

Step 5: Simulation of Gas/Water Two-Phase flow in 3D using CMG

The 2D CMG model parameters were used as a basis for the 3D model. The need for building a 3D model could account for many different aspects that the 2D model couldn't address. The model is a 19x19x10 and the same test case was run with the exact

same parameters to see the effect of adding 9 additional layers. The simulation model represented the hydraulic fracture by a thin column that had the properties of the hydraulic fracture. The well in this case was draining from the hydraulic fracture only.

The 3D model results matched almost exactly with the 2D model match. The difference between the two models is that, the 2D model has 1 layer which is 300 ft while the 3D model has 10 layers that are 30 ft each. Plotting the 3D two-phase model against the 2D two-phase model gave a perfect match except for a small period in the early time as shown in Fig. 4.5.

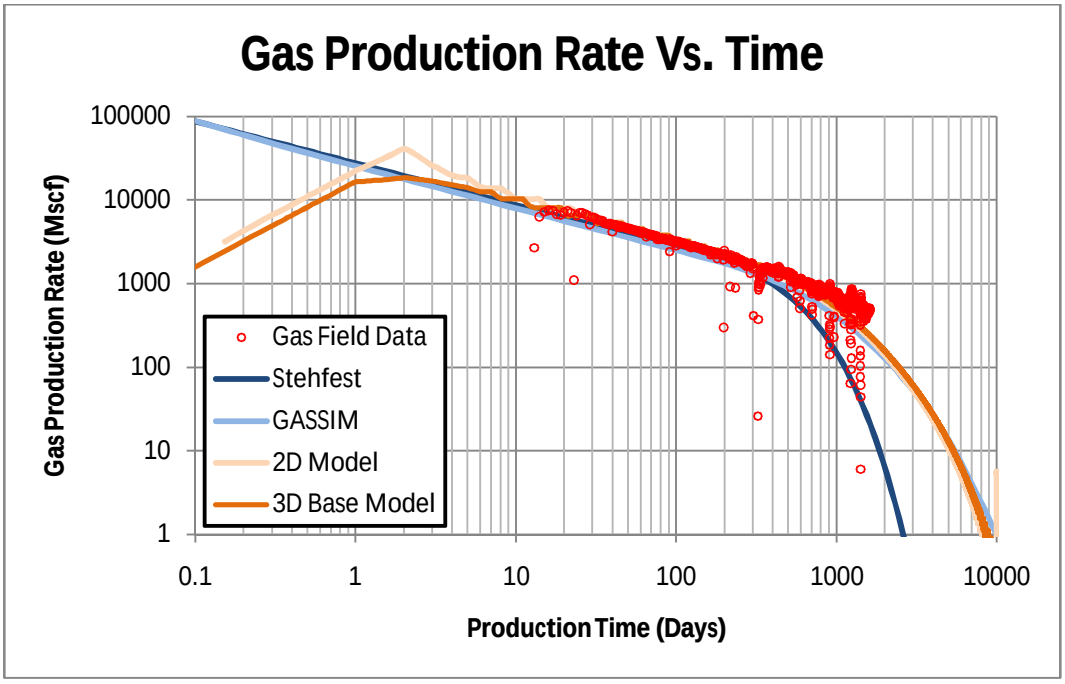

Fig. 4.5 - 3D model creation and comparison with the 2D model. Both models show a very good match with a few differences at very early time.

4.3. Relative Permeability

Relative permeability is the ratio of the effective permeability of a particular fluid at a particular saturation to absolute permeability of that fluid at total saturation. Since only production data were accessible, relative permeability sets were created manually for a shale gas formation that is water wet.

There are two relative permeability set curves in this research, one for the matrix formation, and the other for the hydraulic fracture. The hydraulic fracture relative permeability curve were represented by two straight lines crossing to account for gravity segregation. Gravity segregation is basically the tendency of fluids to stratify into different layers because of gravity forces. In gravity segregation, the heaviest fluid settles near the bottom and the lightest fluid rises to the top.

4.4. Pressure Profile for Base 2D Case

The 2D model which has 19x19x1 CMG simulator case was run, and the pressure profile was taken at different time steps in order to ensure that the model works accurately and according to the scenario it was built for.

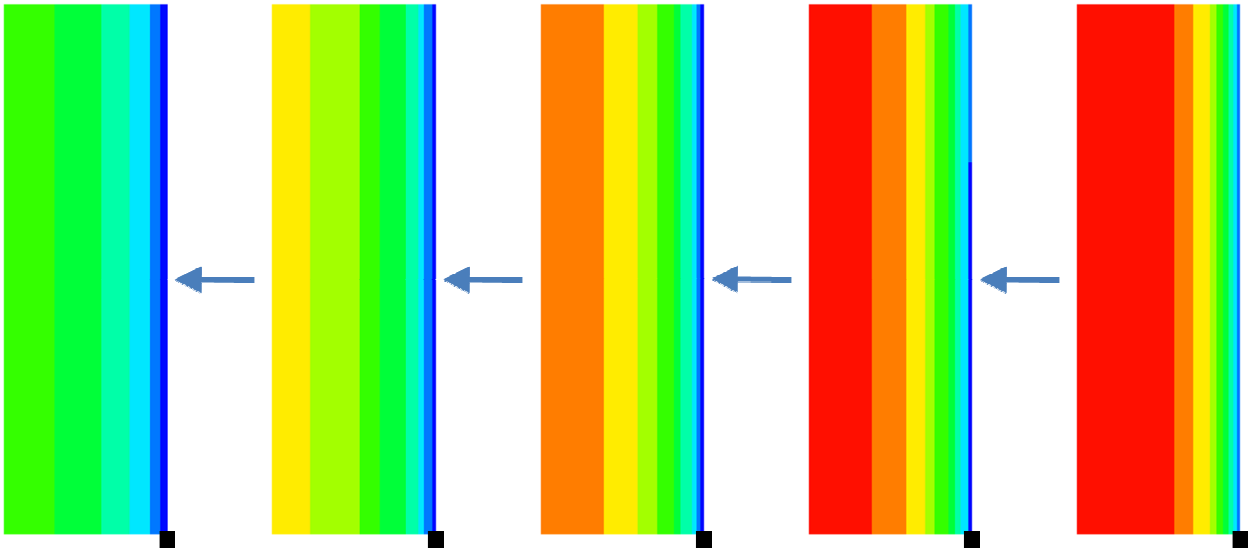

Fig. 4.6 - 2D base case pressure showing pressure drop behavior which indicates gas depletion direction from the matrix formation towards the fracture

The above pressure profile proves that the base 2D case model is accurately capturing the intended flow behavior. Fig. 4.6 shows that the pressure at the hydraulic fracture drops rapidly after one time step to the value of the pwf which pushes the gas in the matrix formation to move into the highly conductive fracture because of the drop in pressure. Fig. 4.6 shows the pressure profile at the segmented model and the rest of the model segments are assumed to behave similarly.

CHAPTER V

SIMULATION MODELS

5.1. Simulation Cases

5.1.1. Test Simulation Case

After verifying the solution models and the simulation models, we developed confidence in our ability to run case studies and do our analysis of the results. The model at this stage perfectly matched the field gas production rate while the water production rate did not match at all.

The purpose of the project is to study the effect of water on the fracture system. So, the first case that was conducted was a test case running the matching 2 Dimensional two-phase case with 100% water saturation in the fractures. All the other parameters with this model were held constant. As previously mentioned, this model is just a segment. All results that were acquired were adjusted to cover the entire well.

Fig. 5.1 and 5.2 show a log-log plot of the gas production rate and water production rate vs. time respectively of the two-phase 2D model against the field data.

Eqn. 5.1 shows the segmented model fracture capacity while Eqn. 5.2 shows the entire well fractures capacity.

$$\omega \times H \times y_e \times \phi_f = 0.1 \times 300 \times 375 \times 0.06 = 675\ ft^3 = 120.2\ BBL \quad \text{.....} \quad (5.1)$$

$$Segment_{Frac\_Capacity} \times N_{Seg} = 120.2 \times 112 = 13{,}462.4\ BBL \quad \text{.....} \quad (5.2)$$

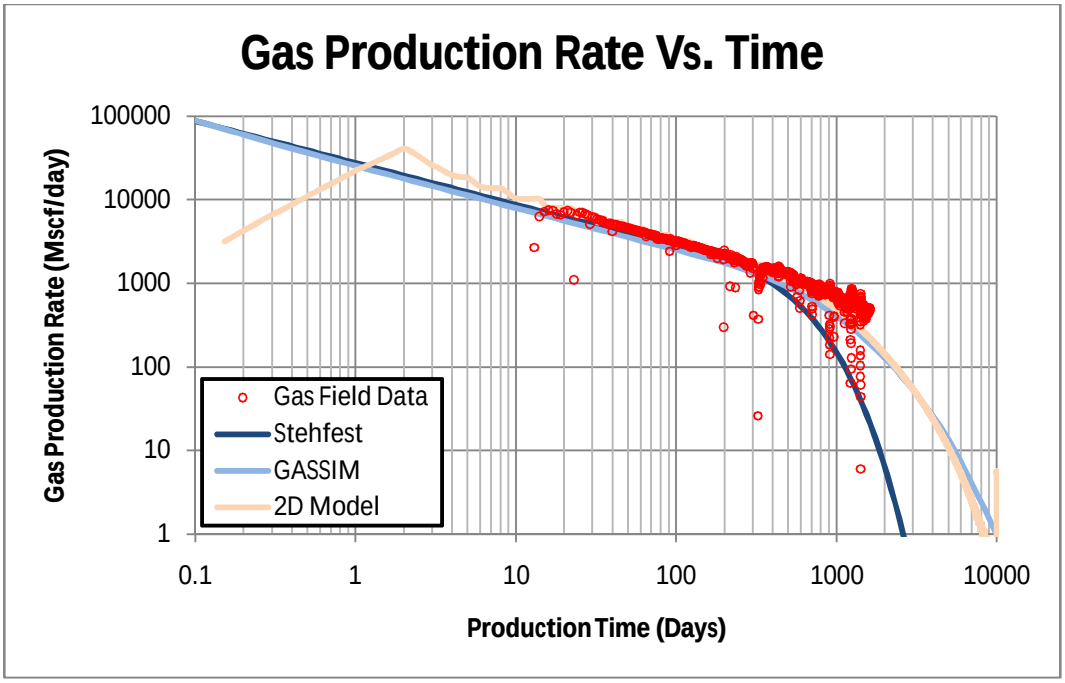

Fig. 5.1 - 2D two phase model running with 100% Sw in the fractures. Gas production match is affected because of water in the fractures

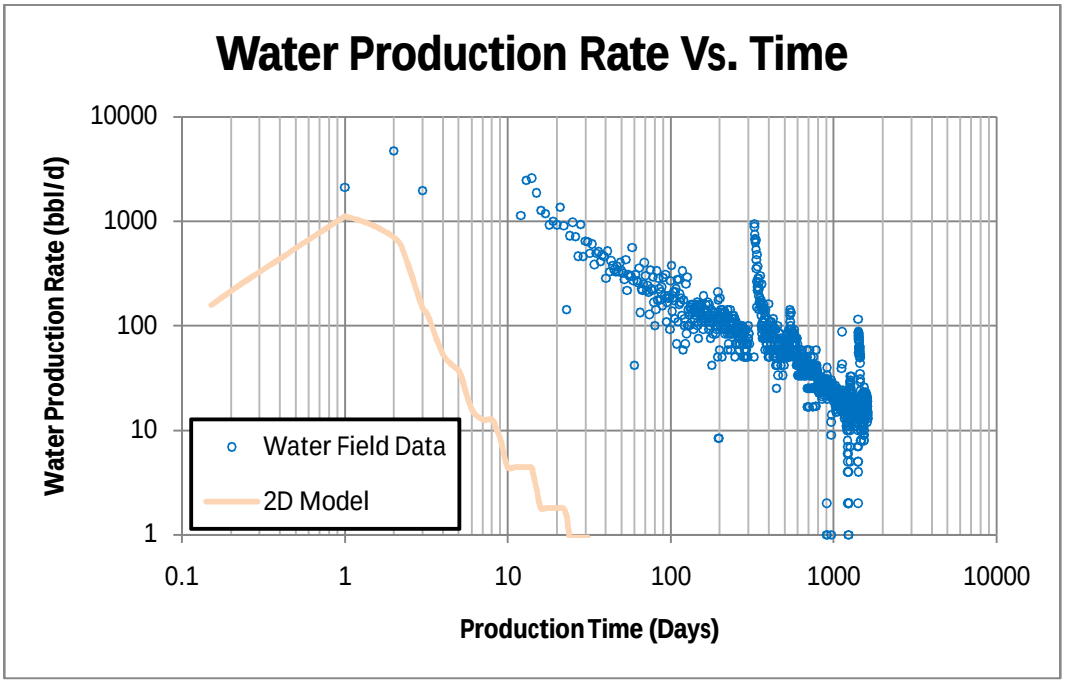

Fig. 5.2 - 2D model running with 100% water in the fracture and 30% Swir in the matrix

5.1.2. Simulation Case # 1

The 2D model produced a good match with the field gas production rate, but the water production rate did not matching well since the only source of water in the current model is the frac water left in the hydraulic fractures after the fracturing job.

Since running the model with 100% water saturation in the fracture system didn't yield enough water, the next simulation scenario was to introduce more water to the model. The first simulation case that was conducted studied the effect of increasing the water saturation in the entire matrix formation. The well in this study has a 30% connate water saturation. This simulation case would study the effect of increasing the water saturation to 40%, 50%, and 60% to see the effect on gas and water production. Fig. 5.3 and 5.4 show the effect of increasing the matrix saturation on the log-log plot of gas production rate and water production rate vs. respectively.

Since the matrix water saturation is increasing, the matrix gas saturation is decreasing. The simulation model is expected to produce more water as the water saturation increases.

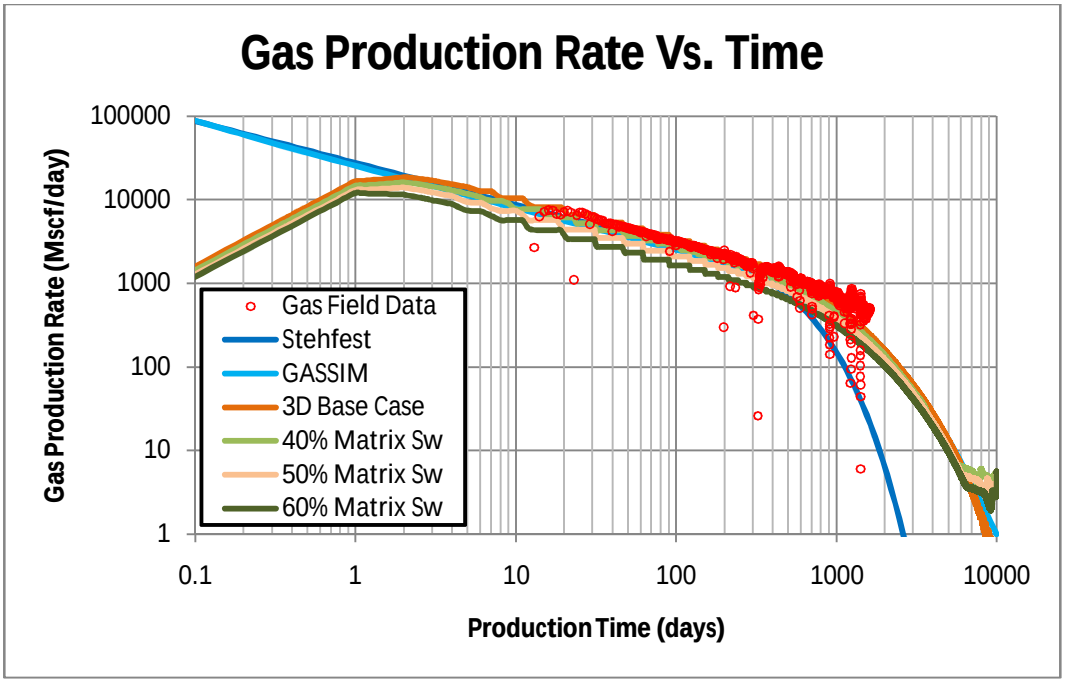

Fig. 5.3 - Effect of increasing matrix Sw on gas production rate. Gas production declines as matrix Sw increases.

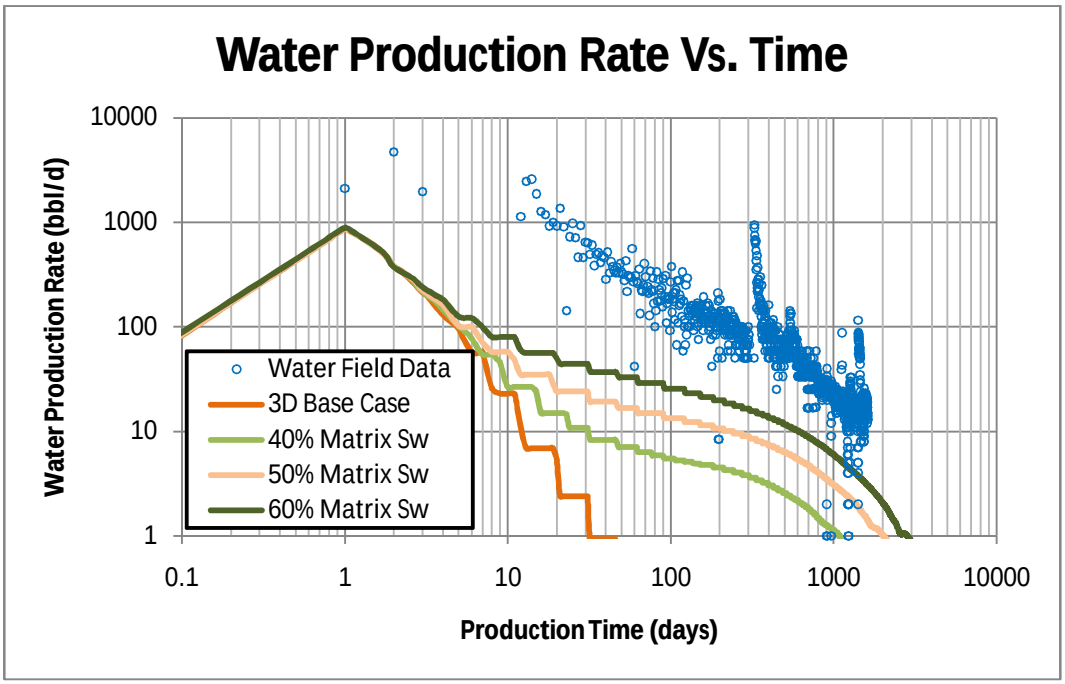

Fig. 5.4 - Effect of increasing matrix Sw on water production rate. Water production increases as matrix Sw increases.

5.1.3. Simulation Case # 2

Increasing the Matrix water saturation is not a realistic way of introducing water to the model. To produce an accurate study, all water sources and their effects on gas and water production needs to be identified.

A new artificial water layer was introduced at the bottom of the segment model as shown in Fig. 5.5. The added bottom water layer is assumed to be fractured as well. While most of the parameters of this layer were unrealistic, the purpose of it was to push the segment model to match the field water production and observe any effect of this bottom water on the fracture system and the overall well performance. The case study well produced more water than initially injected for the hydraulic fracturing job, for that reason, a bottom water layer source is reasonable.

The water layer that was added had properties that allowed water to flow into the well through the hydraulic fracture. Fig. 5.6 and 5.7 show the effect of adding an artifical bottom water layer on the log-log plot of gas production rate and water production rate vs. time respectively.

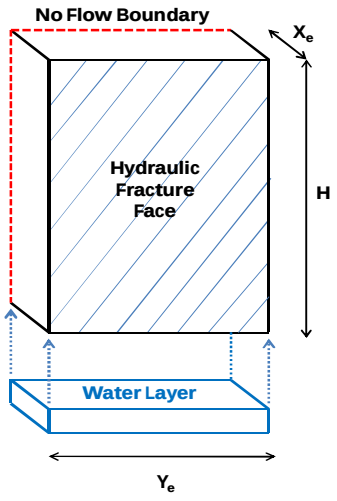

Fig. 5.5 - Basic illustration showing the addition of bottom water to the segmented model. The bottom water is assumed to be fractured as well.

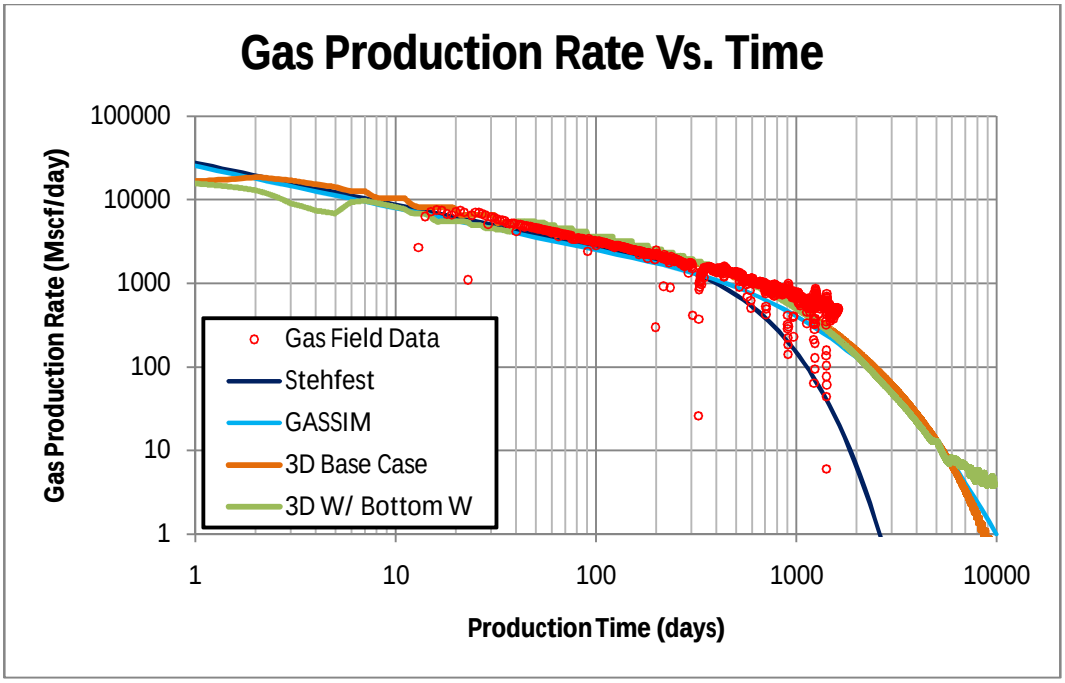

Fig. 5.6 - Effect of adding a bottom water layer. Early time was affected only.

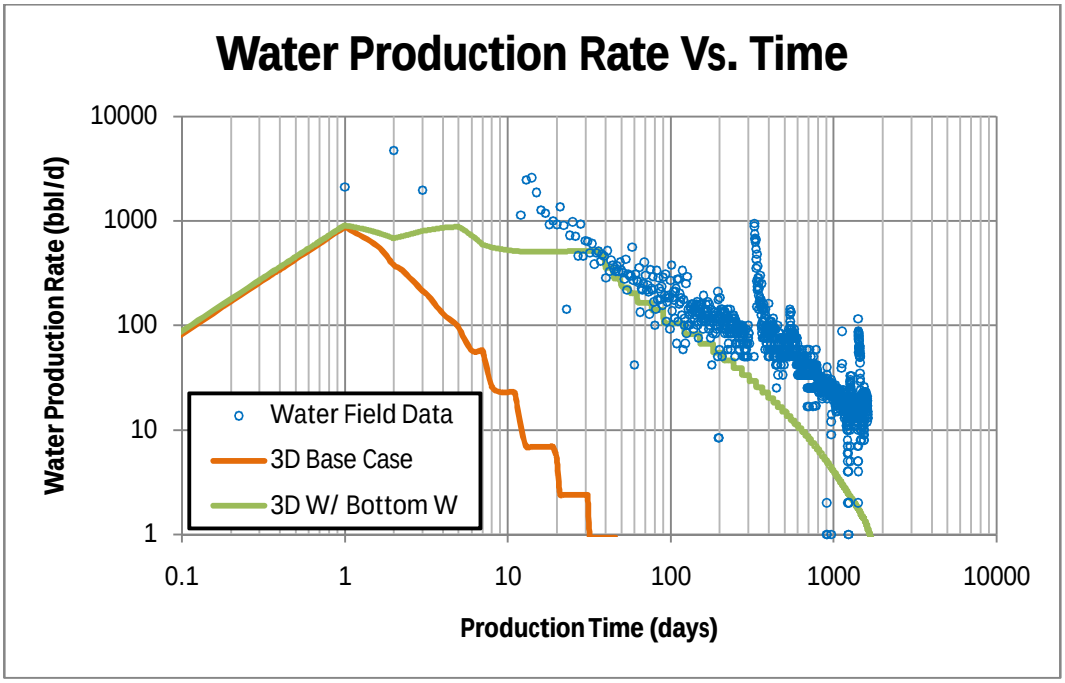

Fig. 5.7 - Adding a bottom water provided the simulation model with the needed water.

5.1.4 Simulation Case # 3

Adding a bottom water layer for the model allowed the model to produce more water than the base simulation case, but that bottom water layer had artificial properties to allow the water to flow through the fractures. The next scenario to be simulated is to simulate a fluid invasion around the hydraulic fractures.

Since we didn't have much fracture data for fracture diagnostic work, in this simulation case we assumed that fluid invades and damages the area surrounding the fractures. Fig. 5.8 shows a possible scenario of water getting trapped around the hydraulic fracture as proposed by **Penny et. al (2006)**. When simulating this case, there will be some frac water trapped around the fracture due to capillary pressure. This scenario was conducted since there is about 91% of fracture water left in the formation after the frac job is over. It is assumed that the invading frac water has the same properties as formation. There would be some areas that are less invaded with water which allows gas to flow from the reservoir to the wellbore through the fractures.

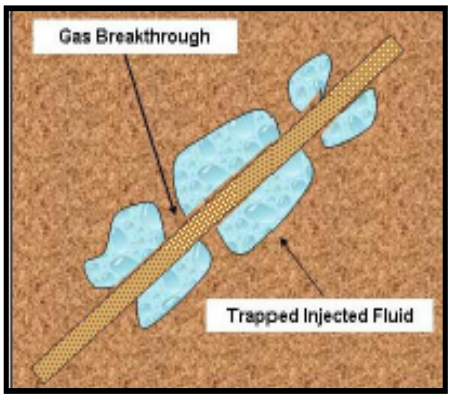

Fig. 5.8 - Frac Water trapped around the hydraulic fracture, Penny et. al

One possible error with this method would be simulating one fracture segment and assuming that water invasion surrounding the fracture is the same throughout the entire well. Since we are studying different scenarios and behaviors, this error would be ignored because there is no way in knowing how fluids invade the area surrounding the fracture, or to what extent, or if it occurs over the entire well. Different water invasion scenarios were simulated using a 3D CMG model.

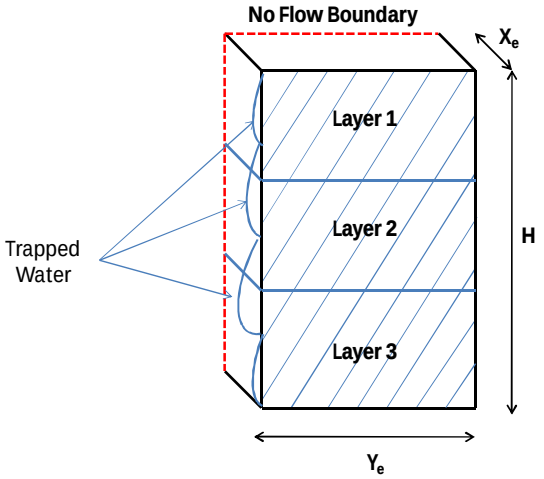

Fig. 5.9 - Segmented model frac water trapped around the hydraulic fracture

The first simulation scenario that was conducted studied the effect of blocking about 53% across all layers of the gas flow due to the invading frac water surrounding the hydraulic fracture. Table 5.1 shows all the water invasion scenarios conducted, the blocked length, and the allowed flow percentage.

Fig. 5.9 shows a general illustration about the segmented model and a random scenario of water blocking some parts around the hydraulic fracture. The figure shows

only 3 layers, while the actual simulation model has 10 layers. This Figure was shown to explain how the frac water invasion was modeled in this case.

Table 5.1 - Frac Water Invaded/Blocked Scenarios				
Scenario #	Ye (ft)	Blocked Length (ft)	% Blocked Length	% Flow Allowed
1	173.5	91.90	52.97	47.03
2		111.90	64.50	35.50
3		51.90	29.91	70.09
4		40.00	23.05	76.95
5		20.00	11.53	88.47
6		15.00	8.65	91.35
7		10.00	5.76	94.24
8		Random Water Invasion		
9		Random Water Invasion		

Fig. 5.10 and 5.11 show the results of all the water invasion scenario on a log-log plot of the gas production rate and water production rate vs. time respectively.

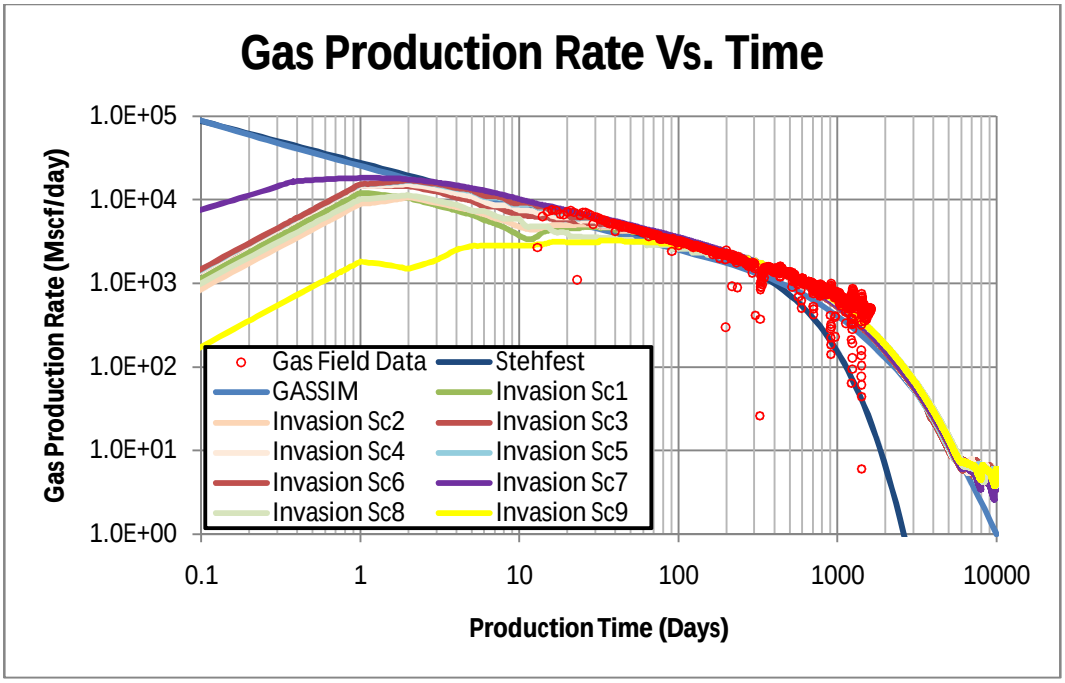

Fig. 5.10 - Effect of trapped frac water around the hydraulic fracture. The plot shows a decrease in gas production as a result of water blockage around the fractures.

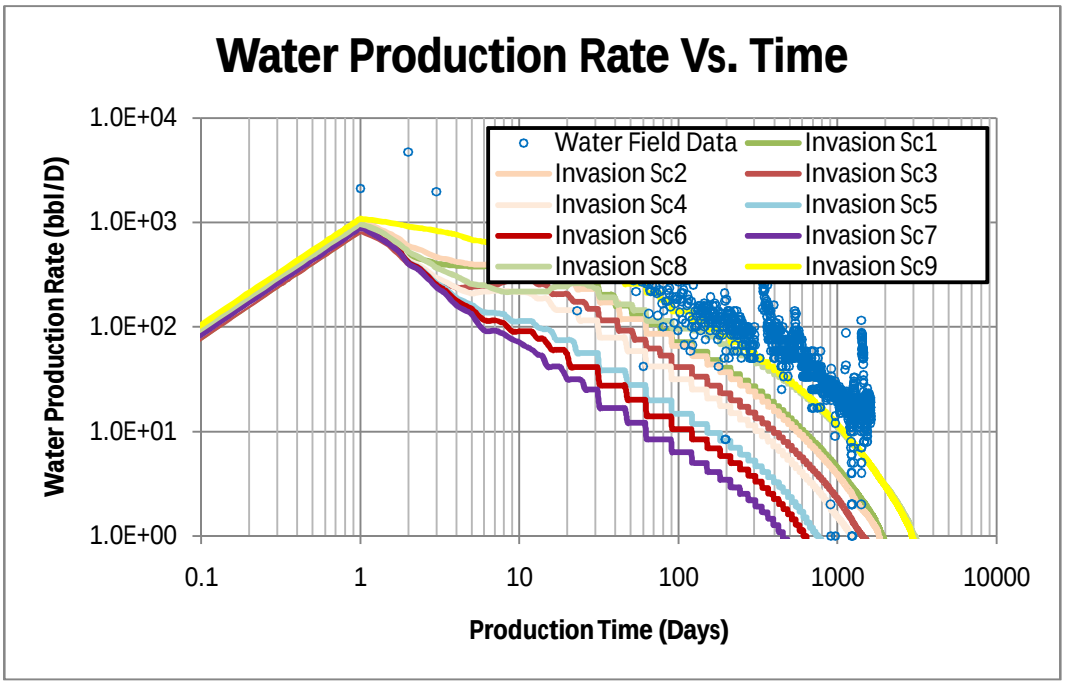

Fig. 5.11 - Effect of trapped frac water around the hydraulic fracture. The plot shows an increase in water production as a result of water invasion around the fractures.

5.1.5. Simulation Case # 4

To further investigate the effect of frac water, a few simulation runs were made by filling one entire layers with water. This simulation case would be appropriate in showing the model accuracy as it should show gravity effect depending on which case is being run and which layer is invaded with water.

Using the 3D model, a simulation case was conducted to see the effect of water invading a whole layer. The 3D model has 10 layers, each layer is a 30 ft. 10 Simulation runs were run, the only difference between these runs was the water saturation. Each run would have a different individual layer totally filled with water while the rest of the layers had connate water saturation. For example, Simulation scenario 1 had 100% water saturation in the first layer and simulation scenario 2 had 100% water saturation in the second layer and so on.

All the parameters for the ten layers were exactly the same, and the rest of the parameters in the model were the same as the previous runs.

Fig. 5.12 and 5.13 show the results of single layer total water invasion on the log-log plot of gas production rate and water production rate vs. time respectively.

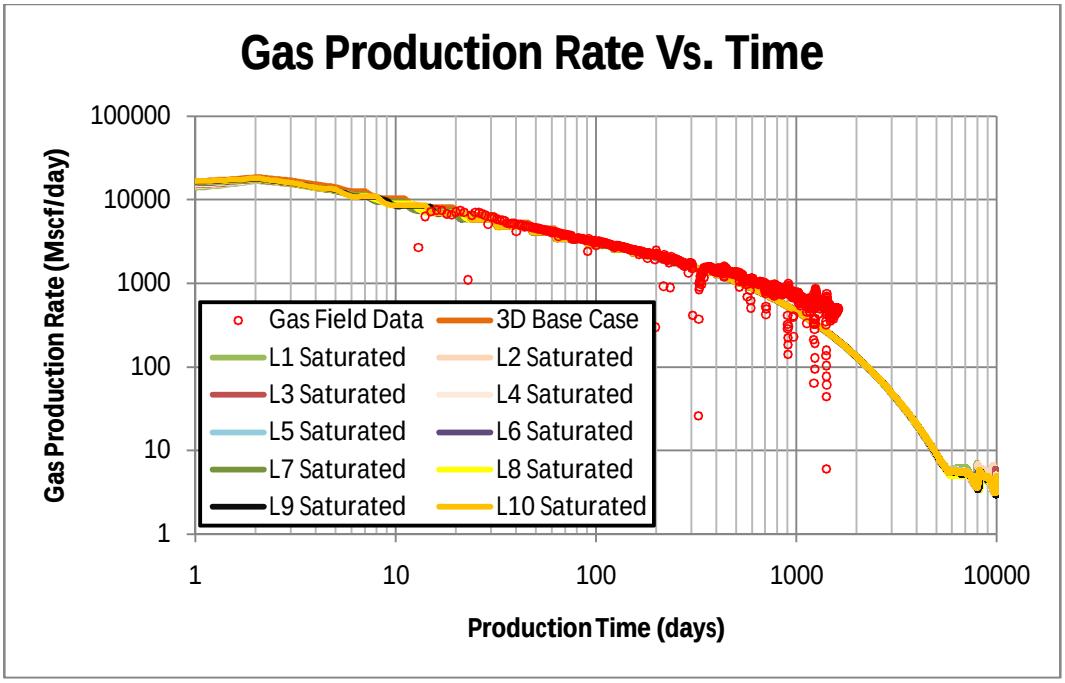

Fig. 5.12 - Effect of single layer total water invasion, gas production rate

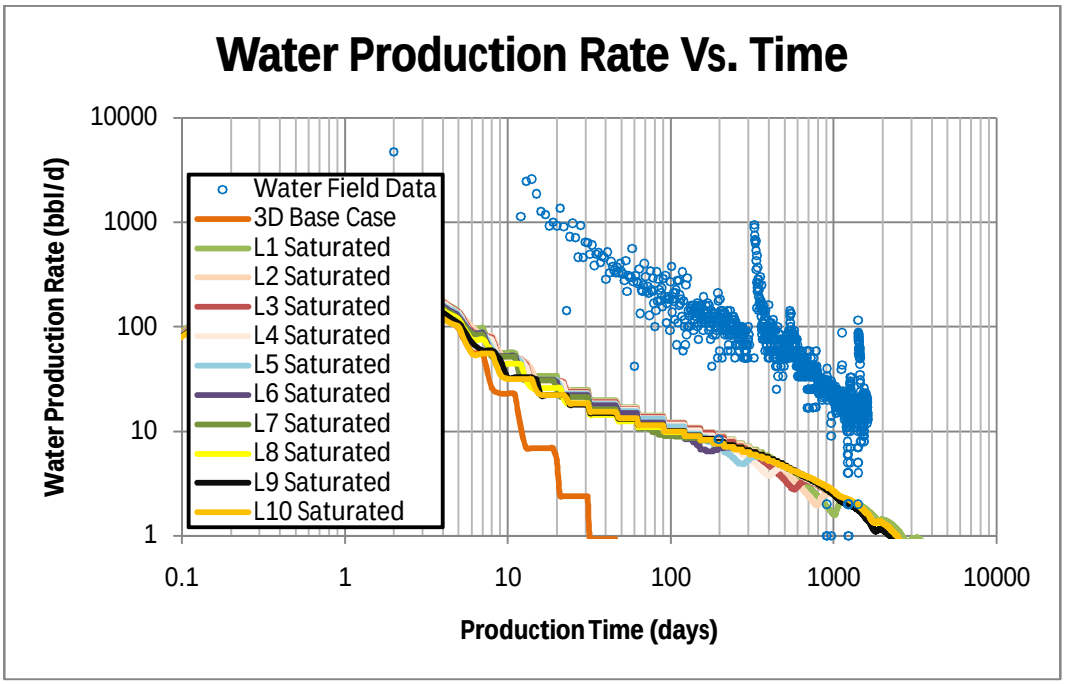

Fig. 5.13 - Effect of single layer total water invasion, water production rate

The previous simulation cases shows that there are minor differences regarding which layer is being invaded by water. These differences are small for a few reasons such as the very tight formation, the mobility of the water, and the fracture conductivity and all of these factors combined doesn't allow for much water production. Fig. 5.14 is the same as Fig. 5.13 but with a different scale to clearly show the gravity effect when fully saturating an individual layer with water. Note that Fig. 5.14 doesn't show 3D Base case model.

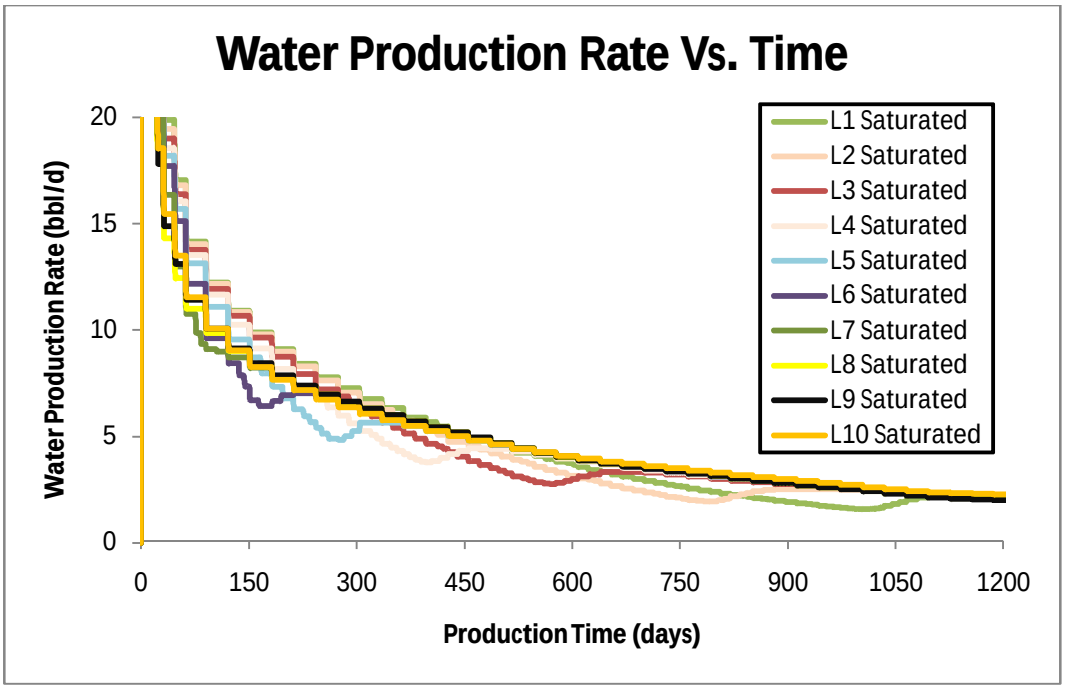

Fig. 5.14 - Simulating single total layer water invasion. The differences shown between all the scenarios are a clear effect of gravity since the only difference between these scenarios is the elevation.

5.1.6. Simulation Case # 5

The next case in this study was to see if frac water could totally block gas production. We are assuming that frac water totally invades and damages the area around the fracture.

Using the 3D model, all the grid blocks surrounding the hydraulic fracture were filled with water. The purpose of that was to see if frac water could totally block gas production which is one of the main questions this study addressed.

Table 5.2 shows a summary of the scenarios conducted under this category. It also shows a few scenarios of the extent of how deep the frac water invades into the matrix formation. Fig. 5.15 shows the effect of water totally invading the area surrounding the hydraulic fracture as well as different scenarios simulating different invasion degrees on the gas production while Fig. 5.16 shows the same results on water production.

Table 5.2 - Extent of Water Blocking Fractures

Scenario #	Xe (ft)	Blocked Width (ft)	% Blocked Width
1	53	1.10	2.08
2		2.35	4.43
3		3.85	7.26
4		5.60	10.57
5		7.60	14.34

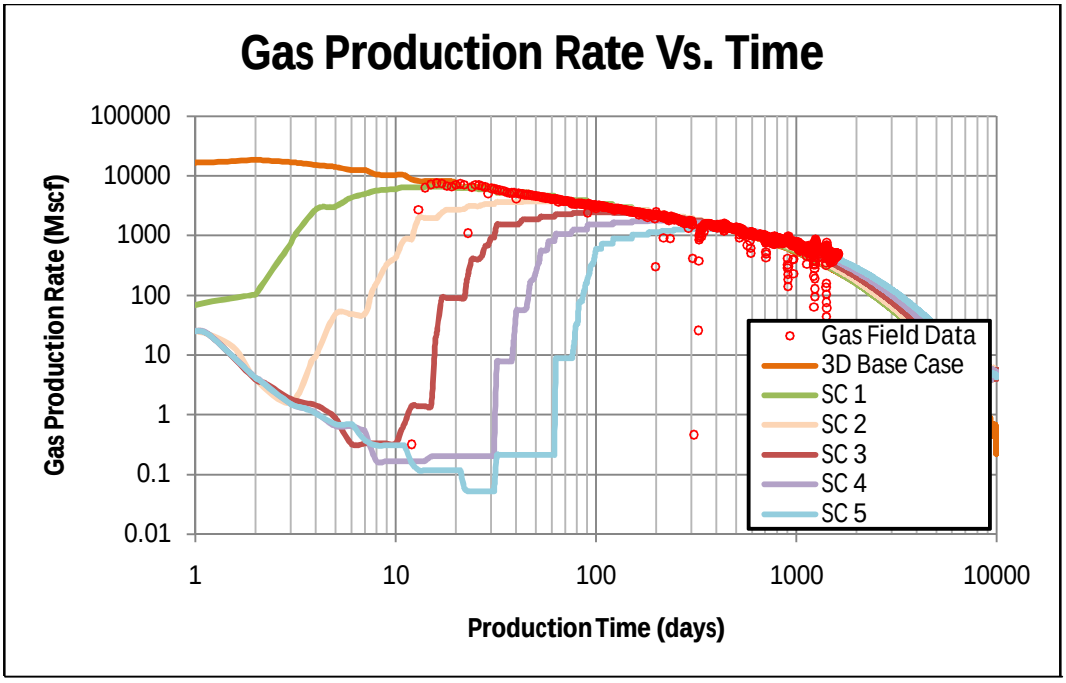

Fig. 5.15 - Effect of frac water totally blocking flow path around the fracture. It can be seen that the extent of the water invasion has a huge impact on the gas production.

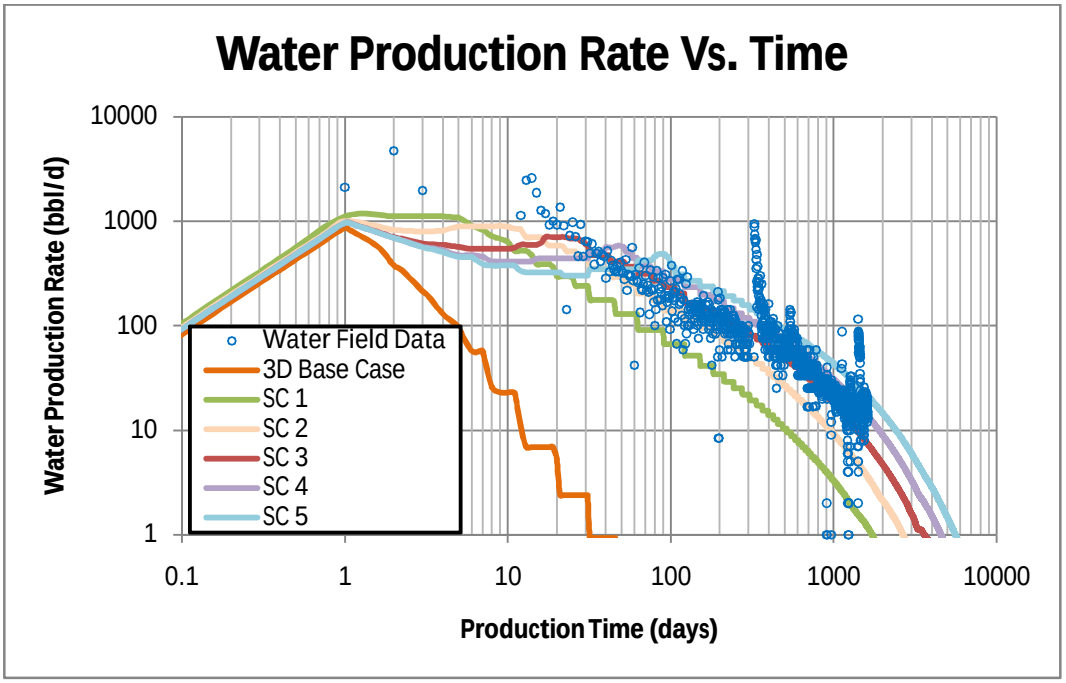

Fig. 5.16 - Effect of frac water totally blocking flow path around the fracture. It can be seen that more water is produced after it was trapped during the fracturing job.

5.1.6. Simulation Case # 6

From the previous simulation cases, sensitivity analysis, and their corresponding results, a more appropriate simulation case that explains possible water sources was developed.

Since the field data shows more water production than the injected frac water for hydraulic fracturing, there is a chance that there is a bottom water layer, and since there are a lot of frac water lost in the formation, there is a high chance that frac water is trapped around the hydraulic fractures.

In this scenario, the 3D Model with the 10 layers was used to simulate a bottom water along with the frac water invading some parts around the fracture. The water in the invaded area around the fracture has the same properties as formation water.

Fig. 5.17 shows the effect of combining a bottom water layer with water invasion on the gas production. Fig. 5.18 shows the water production quality match against the field data for the effect of adding a bottom water with water invasion.

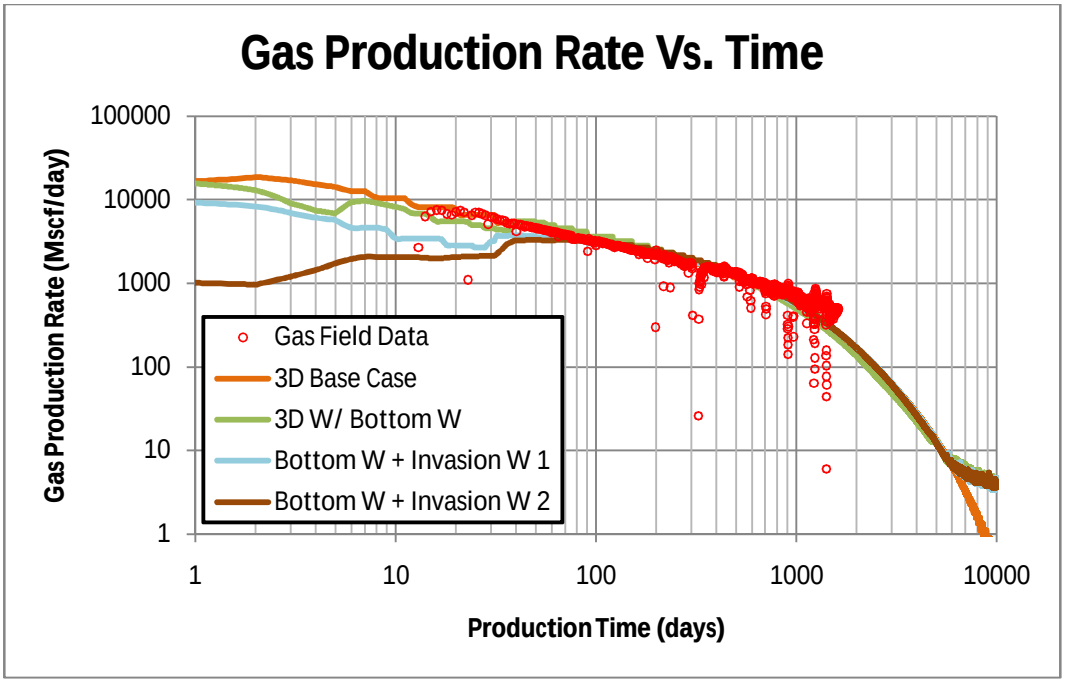

Fig. 5.17 - Effect of adding a bottom water layer combined with water invasion. This plot shows a lower gas production at early time but then matches the field data.

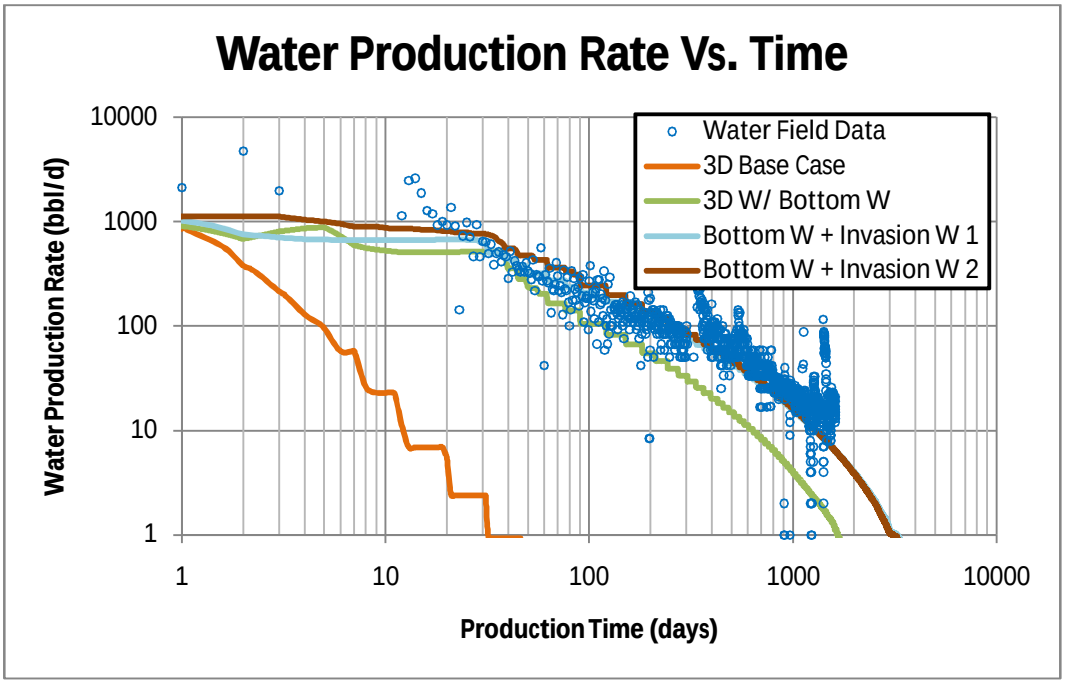

Fig. 5.18 - Effect of adding a bottom water layer combined with water invasion. This combination produces enough water to match the field data.

5.2. Simulation Results

5.2.1. Simulation Case #1: Increasing Matrix Water Saturation

The case study in this research has 30% connate water saturation. Since water behavior and effect is being studied here, it was important to study how formation water behaves. A few simulation cases were conducted by increasing the water saturation to 40%, 50%, and 60%.

Since the water saturation is increasing, the gas saturation is expected to decrease. The simulation model gave the expected results and produced more water as the water saturation increases, but less gas.

5.2.2. Simulation Case #2: Adding a Bottom Water Layer

The purpose of this case was to see if the model is capable of producing enough water to match the field water production. The water in this case leaked into the fracture from a 20 ft bottom water layer which was assumed to be hydraulically fractured.

Adding the bottom water layer showed a minor effect on gas production rate at early time. It is assumed at this case that there is no water invasion or frac water damage around the fracture. The model gave a very good match with the field data, but the problem with this match was that the model overproduced water in the first 10 days and the fact that the bottom water layer had some artificial properties to allow the water to flow.

5.2.3. Simulation Case #3: Trapped Frac Water Around the Fracture

Simulation of this case was the closest scenario to what could have actually happened in the reservoir. There is a lot of frac water left in the formation after the hydraulic fracturing job. Frac water in this scenario would invade/damage the formation face around the hydraulic fractures. Since it is very hard to describe this damage, a few cases were run to demonstrate how this invasion could cause early time skin.
This simulation case allowed the model to produce gas and water simultaneously and gave a very good match with field water production, but the gas production didn't match 100%.

5.2.4. Simulation Case #4: Single Layer Total Water Invasion

It was very important to know if water would behave differently if the frac water damage occurred at different layers. So, the 3D simulation model that has 10 layers was used in this case, and the model was tested with ten different runs where the frac water would happen at a single layer at a time. The results of this simulation case matched the field gas production very well, but the field water production was very poor. It is very important to note that there were small differences between the simulation water production results which is due to gravity. The small differences are because of the very tight formation, mobility of the water, and the conductivity of the hydraulic fracture.

5.2.5. Simulation Case #5: Water Invasion Around the whole Fracture

At this step of the study, knowing if frac water could totally block gas production was crucial. So, in this simulation run, frac water invasion was modeled around the entire length of the hydraulic fracture.

The results of this run shows that gas was unable to pass through the water. The first gas production happened after most of the frac water around the hydraulic fracture was produced and gas was able to pass through the water saturation zone near the hydraulic the fracture.

5.2.6. Simulation Case #6: Water Invasion and Bottom Water

Around 70-90% of frac water is lost to the formation after the hydraulic fracturing job. The field data shows water production more than the injected during the frac job. Since this study is about frac water and its effect, this case had to be run in order to see if frac water is the only contributor to the water production.

The results of this run gives the best match in gas production and water production. We can confirm that frac water is not the only water source that contributed to the water production in this case.

5.3. Analysis of the Results

It is important to note that some of the scenarios conducted in this research were unrealistic and sometimes extreme. In order to study the effects of frac water accurately, a clear understanding of the water sources had to be researched.

After going through the steps to verify the model, it was ready for running different scenarios. The base model was a 3D model 19x19x10 that had an excellent gas production match with the field data, while water production match did not match at all. The base case model was run with 100% water in the fracture and the formation had 30% connate water saturation.

Since access to data was limited, there was no indication of the existence of a bottom water layer in the area of study. So, one of the scenarios conducted was simply adding a bottom water layer to account for the excess water that was being produced but did not include a geological basis. After studying the production data thoroughly and the simulation results from this case, it was concluded that there was a very high chance of a bottom water layer existing under the area of study. There is also a very good geological explanation for this bottom water layer which was addressed early in this research. So, when studying the effect of water, we have to take into consideration the contribution of the bottom water.

Another behavior that was tested was the effect of increasing the water saturation in the matrix formation. The well in this study doesn't show any formation water, but this research studies the effect of water, so it was important to observe how formation water behaves. While this scenario could be considered unrealistic, its effect needed to

be considered. Increasing the water saturation in the formation from 30% (connate water saturation) to 40%, 50%, and 60% basically increased the water production while lowering the gas production.

One of the scenarios that was tested, was a theory that frac water invades and damages random parts around the hydraulic fracture after the fracturing job due to capillary pressure. This case would be the best matching case if bottom water was not considered. Gas and water were flowing into the hydraulic fractures simultaneously. There was no way of knowing what areas were damaged by water, so a few scenarios were conducted by changing the damaged area and differences were noted.

A single whole layer water invasion was tested next. Using the 3D model with 10 layers, a few scenario were simulated. The runs differed in having different layers invaded by water. The results of the ten runs matched the gas production well, but the water production match had minor differences between all the runs.

Surrounding the whole hydraulic fracture with frac water seems extreme especially considering the available field production data. This case was run to see if frac water could totally block the gas production or delay it, and it did. Gas production suffered until most of the water blocking the hydraulic fracture was produced and gas was able to flow.

The previous cases led to the final case which was adding a bottom water layer with the frac water damaging some areas around the hydraulic fractures. This scenario gave the best match, and after studying the data we have, and the simulation results, we

believe that bottom water as well as the frac water damage is the actual mechanism impacting this field case.

It is important to note that we were not able to match the early skin damage that is observed clearly in the field data, but there are a few reasons behind that. This entire simulation study only simulates one segment of the entire well and assumes the rest of the 112 segments behave the same. The limitations in this method appears while simulating frac water invading or getting trapped around the surrounding fracture. There is no way of knowing exactly how fluid gets trapped around the hydraulic fracture.

After running the previous simulation cases, and comparing the base 3D model case with the different simulation cases, we can see that frac water can affect the gas production, and in some cases totally blocking it. Although we didn't simulate the exact early skin damage, we believe that frac water could cause a huge skin on the square root of time plot at early time. If we compare the base 3D case containing water only in the fracture and the 3D case containing bottom water layer and trapped frac water, we can clearly see the gas production rate curve shifting upward indicating the effect of the frac water.

Fig. 5.19 is a plot of the square root of time showing the overall scenarios that tested in this research while Fig. 5.20 shows the early time of the square root of time plot for the scenarios.

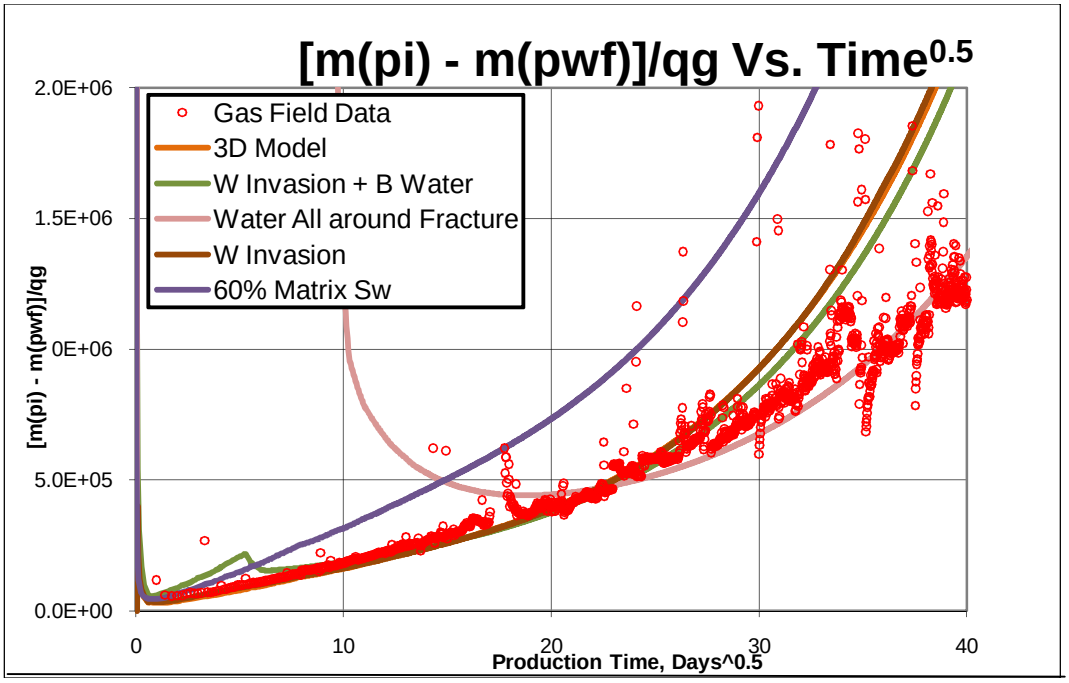

Fig. 5.19 - Square root of time plot showing the overall scenarios that were tested in this research

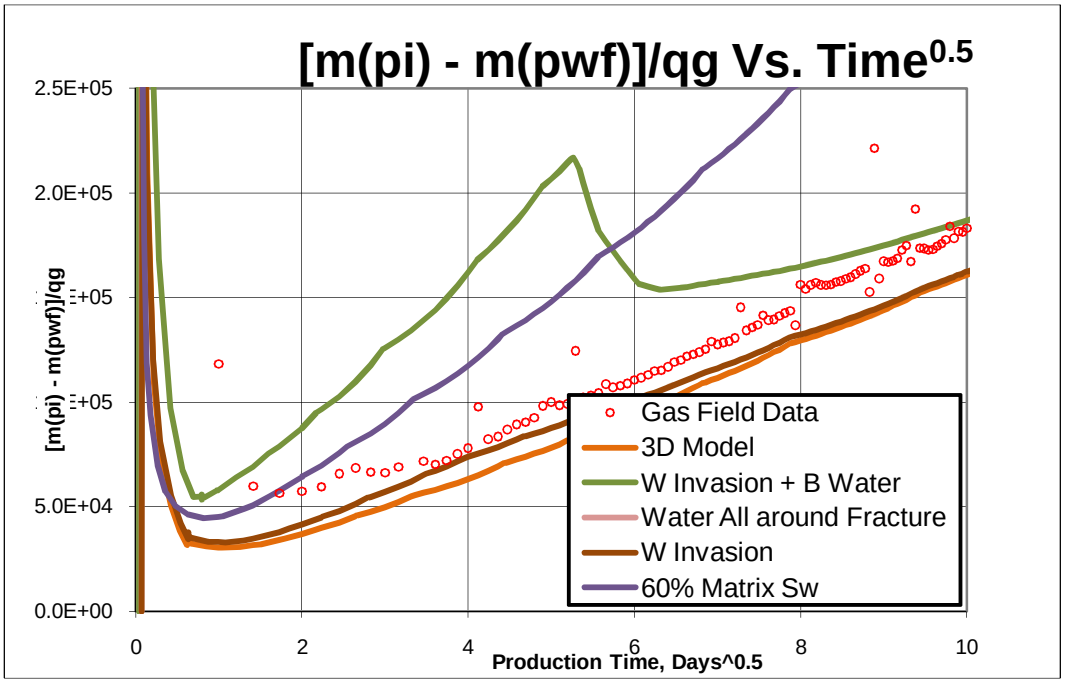

Fig. 5.20 - Square root of time plot comparing the base case with the 3D bottom water and frac water case, notice the shift upwards indicating the effect of frac water

Finally, to clearly show that frac water invasion is a possible cause of huge early time skin, a few different scenarios were conducted. These scenarios differ from each other by having different frac water entrapment behavior. All the other parameters were exactly the same between these runs.

Fig. 5.21 shows the early time data for the water invasion scenarios. It can be clearly seen that water trapped around the hydraulic fracture could cause very huge skin at early time on the square root of time plot because frac water blocks gas flow from the reservoir to the wellbore around the fracture.

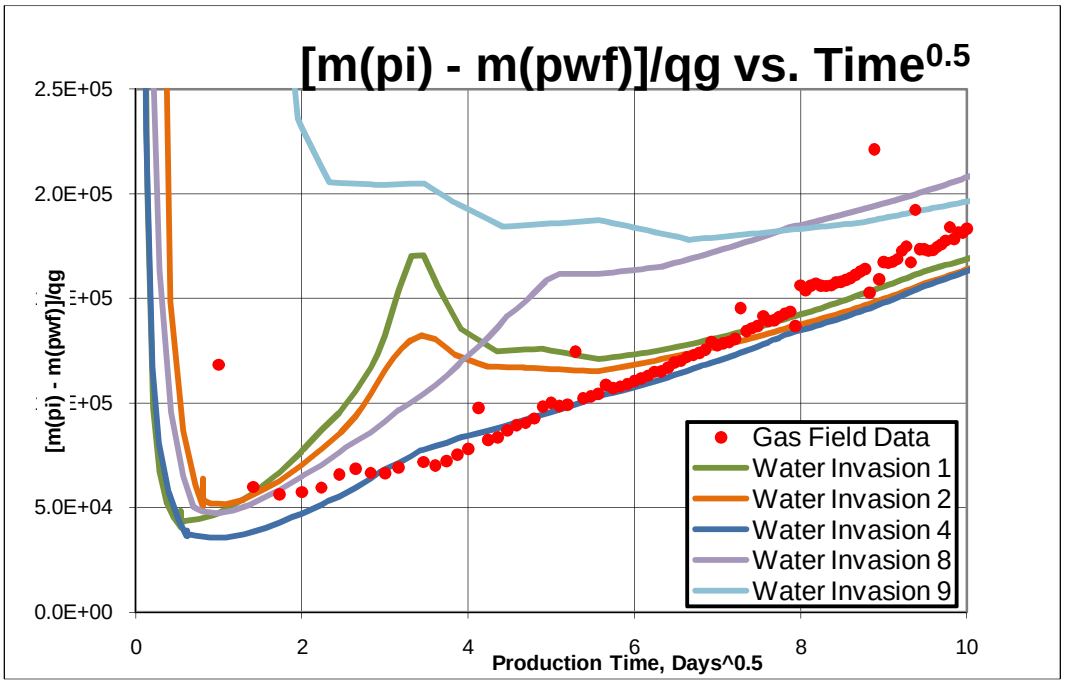

Fig. 5.21 - Different water invasion scenarios causing huge early time skin on the square root of time plot. While field data was not matched very well, a huge intercept was generated through different water invasion scenarios

CHAPTER VI

CONCLUSIONS AND RECOMMENDATIONS

6.1. Conclusions

This study investigates the effect of frac water on the efficiency of the fracture system and its relationship to gas production. This research also tries to relate the huge intercept of the square root of time plot and the frac water that is left in the formation after the hydraulic fracturing job.

Shale gas are very tight formation that requires hydraulic fracturing in order to produce them in commercial quantities. About 70-90% of frac water being left in the formation after the hydraulic fracturing job is common. This frac water may cause some damage around the fracture that could affect or block gas flow between the reservoir and the wellbore.

A 3D reservoir simulation model was built after verifying the accuracy of the model which included building analytical solution models and simple 1D and 2D models. The base 3D model had an excellent gas production rate match with the field data, but the water production was less than half of the water production in the field data Once the 3D model was verified, it was used to run different scenarios to account for the frac water. Many behaviors and trends were observed with different cases. The primary reason behind running a different scenario was to allow the model to produce more water to match the field data. While this research studies the effect of frac water, it was necessary to consider various possible sources of water to analyze its effect accurately.

While some of the scenarios tested were not based on field data, they were considered in order to reach a better understanding of the field. For example, increasing the water saturation in the formation resulted in increasing the water production while lowering the gas production. Adding a bottom water layer that leaked into the hydraulic fracture allowed the model to have good gas and water production rate matches. Trapped frac water randomly around the fracture produced approximately the same amount of water produced by field data, but the gas production suffered a bit. Totally surrounding the fracture with frac water blocked all gas production until most of the water was produced. Finally, trapped frac water randomly around the fracture with a bottom water showed the best match to field behavior.

The main conclusions of this research can be summarized as follows:

1) Invasion of frac water in the matrix surrounding the hydraulic fracture could cause reduced gas flow.

2) Frac water is capable of totally blocking off gas flow from the reservoir to the wellbore and thus lowering the efficiency of the hydraulic fracturing job.

3) Frac water does affects the square root of time plot. We believe that the huge skin at early time could be caused by damage from frac water around the hydraulic fracture.

6.2. Recommendations for Future Work

In order to build on this study and have a better understanding, the following are recommended for future work:

1) Acquire fracture characterization data.

2) Acquire updated water production data.

3) Acquire water injection data during hydraulic fracturing.

4) Acquire updated and specific frac water properties in order to have a better and realistic reservoir simulation.

5) Determine a valid reservoir characterization.

NOMENCLATURE

A_{cm}	total matrix surface area draining into the fracture system, ft^2
A_{cw}	cross-sectional area draining into the fracture system, ft^2
B_{gi}	formation volume factor at initial reservoir pressure, rcf/scf
c_t	liquid total compressibility, psi^{-1}
h	reservoir thickness, ft
k_f	fracture Permeability, md
k_m	matrix Permeability, md
L_1	fracture spacing for Model 1, ft
L_2	fracture spacing for Model 2, ft
$\tilde{m}_4$	slope of the line matching the linear flow data and passing through the origin on the square root of time plot.
$m(p)$	pseudo pressure (gas), psi^2/cp
p_D	dimensionless pressure (transient dual porosity model)
p_i	initial reservoir pressure, psi
p_{wf}	wellbore flowing pressure, psi
q_D	dimensionless rate (transient dual porosity model)
q_{DL}	dimensionless rate based on $A_{cw}^{0.5}$ and k_f (rectangular geometry, dual porosity)
q_g	gas rate, Mscf/day
r_w	wellbore radius, ft

S_{gi}	initial gas saturation, fraction
T	absolute temperature, ^{0}R
t	time, days
t_{DAcw}	dimensionless time based on $A_{cw}^{0.5}$ and k_f (rectangular geometry, dual porosity)
x_e	drainage area length (rectangular geometry), ft
y_{De}	dimensionless reservoir length (rectangular geometry), $y_{De} = y_e / \sqrt{A_{cw}}$
y_e	drainage area half-width (rectangular geometry), equivalent to fracture half-length, ft

Greek Symbols

γ specific gravity

λ dimensionless interporosity parameter

μ viscosity, cp

ω dimensionless storativity ratio

ϕ porosity

Subscript

Ac cross-sectional area to flow

i initial

f fracture system

g gas

m matrix

REFERENCES

Al-Ahmadi, H.A., Almarzooq, A. M. and Wattenbarger, R. A. 2010. Application of Linear Flow Analysis to Shale Gas Wells : Field Cases. Paper SPE 130370 presented at the SPE Unconventional Gas Conference, Pittsburgh, Pennsylvania, USA, 23-25 February.

Arthur, J.D., Bohm, B., Cornue, D. 2009. Environmental Considerations of Modern Shale Gas Development. Paper SPE 122931 presented at the 2009 SPE Annual Conference and Exhibition, New Orleans, Louisiana, USA, 4-7 October.

Barenblatt, G.I., Zheltov, I. P. and Kochina, I.N. 1960. Basic Concepts in the Theory of Seepage of Homogeneous Liquids in Fissured Rocks (Strata), *PMM* (1960) **24 (**5): 852-864.

Bello, R. O. and Wattenbarger, R. A. 2008. Rate Transient Analysis in Naturally Fractured Shale Gas Reservoirs. Paper SPE 114591 presented at the CIPC/SPE Gas Technology Symposium 2008 Joint Conference, Calgary, Alberta, Canada, 16 – 19 June.

Bello, R. O. and Wattenbarger, R. A. 2009. Modeling and Analysis of Shale Gas Production with a Skin Effect. Paper CIPC 2009-082 presented at the Canadian International Petroleum Conference, Calgary, Alberta, Canada, 16 – 18 June.

Bello, R. O. and Wattenbarger, R. A. 2010. Multi-stage Hydraulically Fractured Shale Gas Rate Transient Analysis. Paper SPE 126754 presented at the SPE North Africa Technical Conference and Exhibition, Cairo, Egypt, 14 – 17 February.

Bello, R.O. 2009. Rate Transient Analysis in Shale Gas Reservoirs with Transient Linear Behavior. PhD dissertation, Texas A&M U., College Station, Texas.

El-Banbi, A.H. 1998. Analysis of Tight Gas Wells. PhD dissertation, Texas A&M U., College Station, Texas.

Holditch, S.A. 1979. Factors Affecting Water Blocking and Gas Flow from Hydraulically Fractured Gas Wells, Journal of Petroleum Technology *SPEJ* 31 (12): 1515-1524.

Ibrahim, M. and Wattenbarger, R. A. 2005. Analysis of Rate Dependence in Transient Linear Flow in Tight Gas Wells. Paper CIPC 2005-057 presented at the Canadian International Petroleum Conference, Calgary, Alberta, Canada, 7 – 9 June.

Lewis, A. M. and Hughes, R. G. 2008. Production Data Analysis of Shale Gas Reservoirs. Paper SPE 116688 presented at the SPE Annual Technical Conference and Exhibition, Denver, Colorado, 21 – 24 September.

Mattar, L., Gault, B., Morad, K., Clarkson, C. R., Freeman, C. M., Ilk, D. and Blasingame, T. A. 2008. Production Analysis and Forecasting of Shale Gas Reservoirs: Case History-Based Approach. Paper SPE 119897 presented at the 2008 SPE Shale Gas Production Conference, Fort Worth, Texas, 16 – 18 November.

Medeiros, F., Ozkan, E. and Kazemi, H. 2008. Productivity and Drainage Area of Fractured Horizontal Wells in Tight Gas Reservoirs. 902 – 911. Paper SPE-108110-PA presented at Rocky Mountain Oil and Gas Technology Symposium, Denver, Colorado, 16-18 April.

Montgomery, S.L., Jarvie, D.M., Bowker, K.A. and Pollastro, R.M. 2005. Mississippian Barnett Shale, Fort Worth Basin, North-central Texas: Gas-shale Play with Multi-trillion Cubic Foot Potential. AAPG Bulletin, V. **89 (**2): 155-175.

Palisch, T.T., Vincent, M.C. and Handren, P.J. 2008. Slickwater Fracturing : Food for Thought. Paper SPE 115766 presented at the 2008 SPE Annual Technical Conference and Exhibition, Denver, Colorado, USA, 21-24 September.

Penny, G. S., Pursley, J. T. and Clawson, T. D. 2006. Field Study of Completion Fluids To Enhance Gas Production in the Barnett Shale. Paper SPE 100434 presented at the 2006 SPE Gas Technology Symposium, Calgary, Alberta, Canada, 15-17 May.

Stehfest, H. 1970. Algorithm 358 – Numerical Inversion of Laplace Transforms, *Comm. ACM* **13 (**1): 47-49.

Wang, J. Y., Holditch, S. A. and McVay, D. A. 2009. Modeling Fracture Fluid Cleanup in Tight Gas Wells. Paper SPE 119624 presented at the 2009 SPE Hydraulic Fracturing Technology Conference, Woodlands, Texas, USA 19-21 January.

Warren, J.E. and Root, P.J. 1962. The Behavior of Naturally Fractured Reservoirs. Paper SPE 426 presented at the 1962 Fall Meeting of the Society of Petroleum Engineers, Los Angeles, California, 7 – 10 October.

APPENDIX A

MULTIPHASE DIFFUSIVITY EQUATION

Martin's Equation: $$\nabla^2 P = \frac{\phi C_t}{\lambda}\frac{\partial P}{\partial t}$$

Total Rock Compressibility: $$C_t = -\frac{S_o}{B_o}\frac{\partial B_o}{\partial p} - \frac{S_w}{B_w}\frac{\partial B_w}{\partial p} - \frac{S_g}{B_g}\frac{\partial B_g}{\partial p}$$

Total Fluid Mobility: $$\lambda = \lambda_o + \lambda_w + \lambda_g$$

$$\lambda = \frac{k}{\mu}$$

$$\lambda = \left(\frac{k}{\mu}\right)_o + \left(\frac{k}{\mu}\right)_w + \left(\frac{k}{\mu}\right)_g$$

Looking at the two-phase diffusivity equation for a system containing gas and water:

Martin's Equation: $$\nabla^2 P = \frac{\phi C_t}{\lambda}\frac{\partial P}{\partial t}$$

Total Rock Compressibility: $$C_t = -\frac{S_w}{B_w}\frac{\partial B_w}{\partial p} - \frac{S_g}{B_g}\frac{\partial B_g}{\partial p}$$

Total Fluid Mobility: $$\lambda = \lambda_w + \lambda_g$$

$$\lambda = \left(\frac{k}{\mu}\right)_w + \left(\frac{k}{\mu}\right)_g$$

$$\mu_g \approx 0.01$$

$$\mu_w \approx 1$$

$$\therefore \left(\frac{k}{\mu}\right)_w < \left(\frac{k}{\mu}\right)_g$$

APPENDIX B

GASSIM CODE PARAMETERS

CASE	\\pe-admin\home\bob.wattenbarger\My Documents\COURSES\Latest Excel Programs\Gassim6\Case6_hydr fracture.dat													
CMNT	case6													
CMNT														
CMNT	Well	containing	vertical	hydraulic	fractures									
CMNT	Finite	conductivit	fracture	(Cinco-L	et	al)								
CMNT	Slightly	compressi	fluid											
CMNT														
CMNT	Wellbore	storage	and	skin	effects	are	neglected.							
CMNT														
CMNT														
CMNT	Single	Value	Input	Data										
IMAX	19													
JMAX	19													
CMNT														
CROC	0.000015													
PREF	2950													
NEWT	1													
CMNT														
CMNT	Bo,	rcf/scf	Visc,	cp										
SWAT	0.3													
T	610													
GRAV	0.65													
END														
CMNT	Grid	Input	Data											
CMNT	Areal	grid	system,	quadrant	model	-->	xe=ye=12!	ft.						
CMNT														
CMNT														
CMNT	xe/xf	=	10	---->	xf	=	1250/10	=	125	ft				
CMNT	Geometruc	spaced	for	40183	of	the	xf,	uniform	fine	grids	for	the	remaining	xf.
CMNT	Geometric	spaced	grids	from	the	fracture	tip	to	the	outer	boundary	of	reservoir.	
CMNT	Cells	1	to	29	are	fractures,	30	to	46	are	reservoir			
DELX	-1		1.181869		53									
	0.1	0.5	0.590934	0.698407	0.825426	0.975545	1.152966	1.362655	1.61048	1.903376				
	2.249541	2.658662	3.14219	3.713657	4.389056	5.187289	6.130695	7.245678	8.563442					
DELY	-1		1.31452		173.5									
	0.1	0.4	0.525808	0.691185	0.908577	1.194343	1.569989	2.063782	2.712883	3.56614				
	4.687764	6.162161	8.100286	10.64799	13.997	18.39934	24.18631	31.79339	41.79306					
CMNT														
CMNT	Global	Data												
H	300													
KX	0.00015													
KY	0													
PHI	0.06													
POI	2950													
CMNT														
CMNT	Fracture													
WIND	1	1	1	18										
PHI	0.03													
KX	100000													
KY	1000													
END														
CMNT	Schedule	Data												
CMNT														
CMNT														
CMNT	Well	No.	i	-	location	j	-	location	skin					
NAME	1	1	1	0										
CMNT	Well	No.	scf/D											
PWF	1	500												
ALPH	1.2													
DELT	0.01													
DTMX	5000													
WELL	1													
PMAP	1													
TIME	10000													
CMNT	\\pe-admin\home\bob.wattenbarger\My Documents\COURSES\Latest Excel Programs\Gassim6\Case6_hydr fracture.dat													

APPENDIX C

CMG 3D 19x19x10 BASE CASE CODE

```
GRID VARI 19 19 10
KDIR DOWN
DI IVAR
 5*4.08 4 3.75 3.5 3.25 3 2.75 2.5 2.25 2 1.75 1.5 1.25 1.1 0.1
DJ JVAR
 51.9 40 20 15 10 6 5 4 3.5 3 2.75 2.5 2.25 2 1.75 1.5 1.25 1.1 1
DK ALL
 3610*30
DTOP
 361*6000
**$ Property: Permeability I (md)   Max: 0.00015  Min: 0.00015
PERMI CON      0.00015
 *MOD
  19:19    1:19    1:10   = 100
**$ Property: NULL Blocks  Max: 1  Min: 1
**$  0 = null block, 1 = active block
NULL CON           1
 *MOD
   1:18   19:19    1:1   = 0
**$ Property: Porosity  Max: 0.06  Min: 0.06
POR CON         0.06
*MOD
  19:19    1:19    1:10   = 0.03
**$ Property: Permeability J (md)   Max: 0.00015  Min: 0.00015
PERMJ CON      0.00015
```

```
*MOD
  19:19    1:19    1:10   = 100
**$ Property: Permeability K (md)   Max: 0.00015  Min: 0.00015
PERMK CON      0.00015
*MOD
 19:19    1:19    1:10   = 100
**$ Property: Pinchout Array  Max: 1  Min: 1
**$  0 = pinched block, 1 = active block
PINCHOUTARRAY CON           1
PRPOR 2950
CPOR 1e-6
**---PVT DESCRIPTION SECTION----------------------------------------------------------
MODEL BLACKOIL
TRES 150
PVT BG 1
**$        p       Rs       Bo          Bg      viso       visg
      14.696   3.50522   1.04124     0.207908   3.71326  0.0123408
     27.0496   4.84173   1.04171     0.112797   3.67448  0.0123477
     39.4032   6.24478   1.04222     0.077324   3.63471  0.0123555
     51.7568   7.70392   1.04274    0.0587851   3.59434  0.0123641
     64.1104   9.21186   1.04328    0.0473907   3.55362  0.0123734
      76.464   10.7631   1.04383    0.0396783   3.51278  0.0123831
     88.8176   12.3534    1.0444    0.0341113   3.47195  0.0123934
     101.171   13.9794   1.04499    0.0299039   3.43127  0.0124042
     113.525   15.6383   1.04559    0.0266124   3.39082  0.0124153
     125.878   17.3276    1.0462    0.0239669   3.35069  0.0124269
     138.232   19.0455   1.04682    0.0217943   3.31093  0.0124388
```

150.586 20.7901 1.04745 0.0199782 3.27159 0.012451

162.939 22.56 1.04809 0.0184376 3.23272 0.0124636

175.293 24.3539 1.04874 0.0171141 3.19434 0.0124766

187.646 26.1705 1.0494 0.015965 3.15648 0.0124898

200 28.0088 1.05007 0.0149578 3.11916 0.0125033

500 82.3164 1.07083 0.00561814 2.5647 0.0130128

960 165.588 1.10266 0.00287019 1.71453 0.013794

1720 329.721 1.17057 0.00151023 1.16623 0.015902

2480 509.653 1.24988 0.00103112 0.888095 0.0186551

3000 640.771 1.31073 0.000868734 0.774055 0.0207149

3240 701.287 1.33881 0.000809867 0.721421 0.0216656

4000 902.358 1.43621 0.000690303 0.610561 0.0246139

BWI 1.001420

CVW 0

CW 3.0e-006

DENSITY WATER 62.14

REFPW 14.696

VWI 0.96

GRAVITY GAS 0.65

DENSITY OIL 53.9738

CO 0

CVO 0

**---ROCK-FLUID PROPERTY SECTION----------

ROCKFLUID

RPT 1

SWT

**$ Sw krw krow

0 0 1

```
        0.3         0         1
         .4  0.0476948  0.647059
         .5  0.0969793   0.45787
         .6   0.171701  0.284579
         .7    0.27504  0.133545
         .8   0.384738         0
          1         1         0
SGT
**$        Sg        krg       krog
          0         0         1
       0.05         0         1
        0.1  0.0445151  0.895072
        0.3   0.225755  0.551669
        0.5   0.392687  0.332273
        0.7   0.594595  0.124006
        0.9   0.837838         0
          1         1         0
**$ Property: Rel Perm Set Num  Max: 1  Min: 1
RTYPE CON           1
 *MOD
  19:19    1:19    1:10   = 2
**$ Property: Endpoint Saturation: Connate Water  Max: 0.3  Min: 0.3
SWCON CON          0.3
RPT 2
SWT
**$        Sw       krw       krow
          0         0         1
         .5        .5        .5
```

```
        1       1       0
SGT NOSWC
**$       Sg      krg     krog
        0       0       1
       0.5      .5      .5
        1       1       0
  **---INITIALIZATION SECTION----------
INITIAL
USER_INPUT
PBT 1
**$     Depth       Pb
       6000      200
       6300      200
**$ Property: Pressure (psi)   Max: 2950  Min: 2950
PRES CON        2950
**$ Property: Oil Saturation  Max: 0  Min: 0
SO CON          0
**$ Property: Water Saturation  Max: 0.3  Min: 0.3
SW CON          0.3
 *MOD
  19:19    1:19    1:10   = 0.99
 **---NUMERICAL CONTROL SECTION----------
NUMERICAL
DTMAX 61
DTMIN 0.000001
NCUTS 10
RUN
 **---WELL AND RECURRENT DATA SECTION----------
```

```
DATE 2004 12 11
**$
WELL  'Well-1'
PRODUCER 'Well-1'
OPERATE  MIN  BHP  500.  CONT
OPERATE  MAX  STG  1e+006  CONT
OPERATE  MAX  STW  10.  CONT
**$         rad  geofac  wfrac  skin
GEOMETRY  K  0.1  0.37  1.  0.
PERF  GEOA  'Well-1'
**$ UBA      ff  Status  Connection
   19 19 1  1.  OPEN    FLOW-TO  'SURFACE'
AIMWELL WELLN
TRIGGER 'Trigger-name' ON_WELL 'Well-1' STG-RP > 0.
END_TRIGGER

DATE 2005 1 11.00000
DATE 2005 2 11.00000
DATE 2005 3 11.00000
DATE 2005 4 11.00000
DATE 2005 5 11.00000
DATE 2005 6 11.00000
DATE 2005 7 11.00000
DATE 2005 8 11.00000
DATE 2005 9 11.00000
DATE 2005 10 11.00000
DATE 2005 11 11.00000
DATE 2005 12 11.00000
```

DATE 2006 1 11.00000

DATE 2006 2 11.00000

DATE 2006 3 11.00000

DATE 2006 4 11.00000

DATE 2006 5 11.00000

DATE 2006 6 11.00000

DATE 2006 7 11.00000

DATE 2006 8 11.00000

DATE 2006 9 11.00000

DATE 2006 10 11.00000

DATE 2006 11 11.00000

APPENDIX D

RANDOM WATER INVASION PRESSURE PROFILES

a) Water Invasion Scenario a (Random Frac Water Entrapment around Hydraulic Fracture)

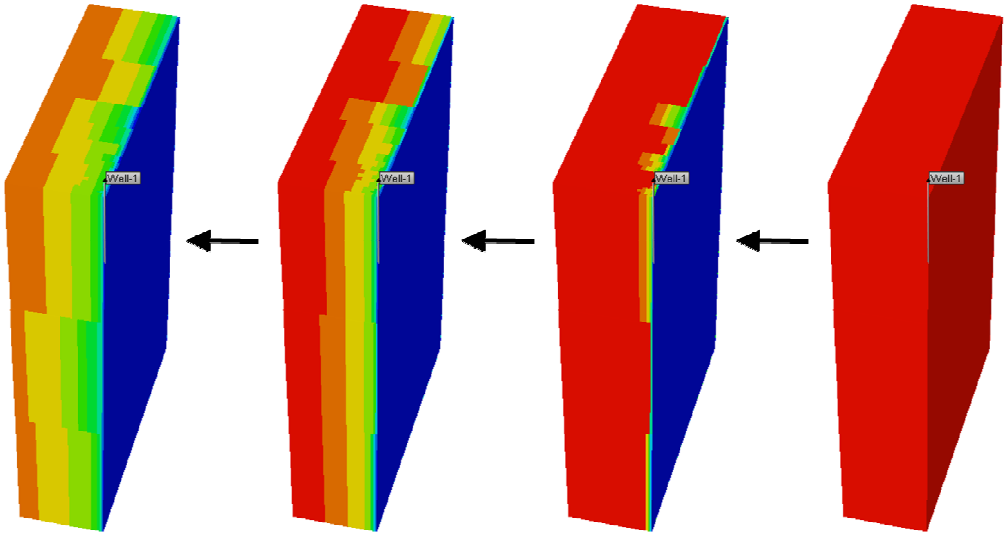

b) Water Invasion Scenario b (Frac Water Invading Layer 1 by the Hydraulic Fracture)

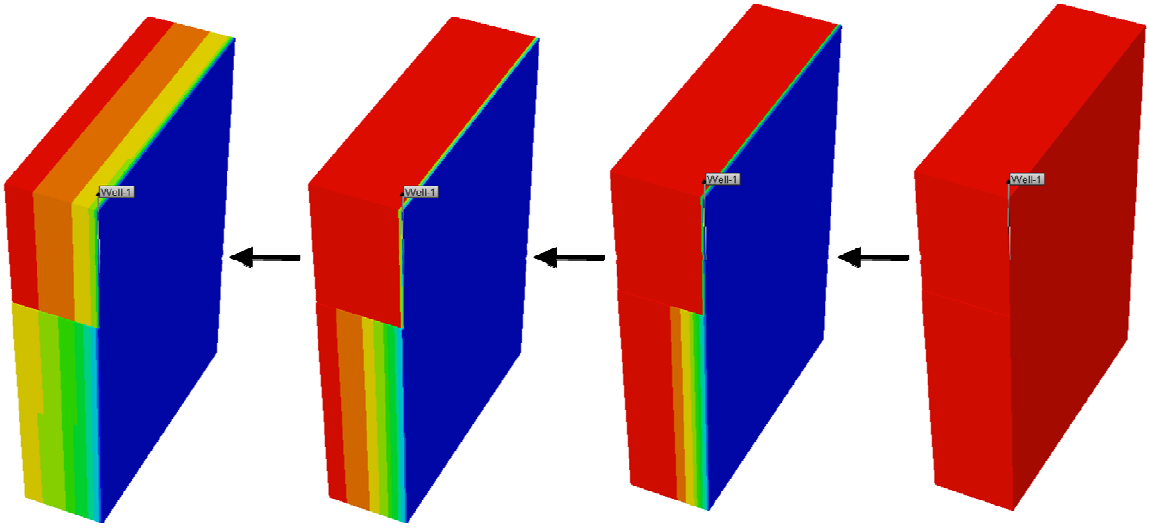

c) Water Invasion Scenario c (Random Frac Water Entrapment around Hydraulic Fracture)

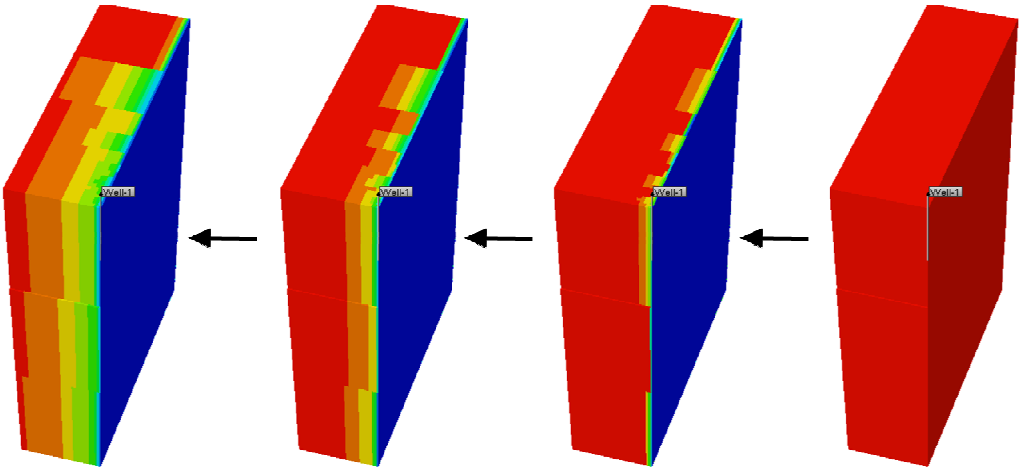

d) Water Invasion Scenario d (Random Frac Water Entrapment around Hydraulic Fracture)

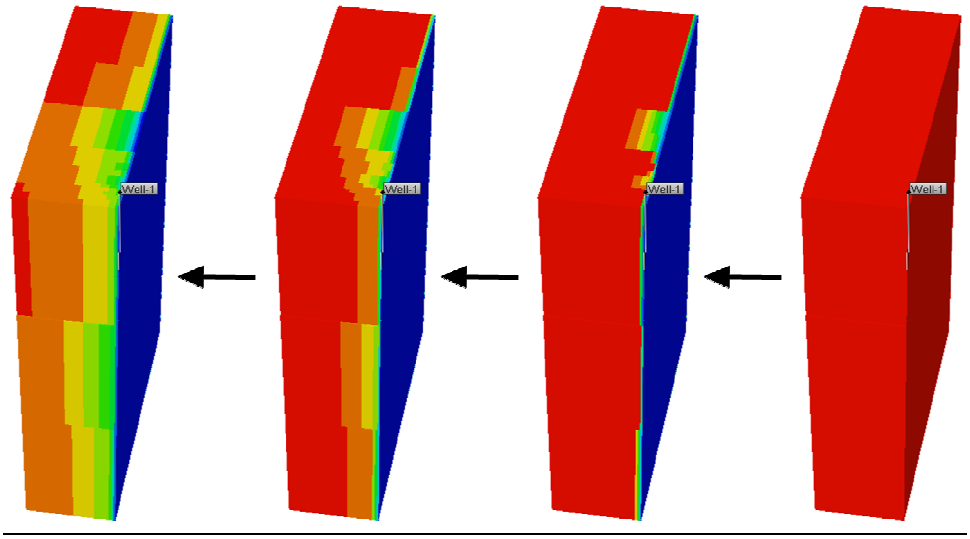

APPENDIX E

WELL 314 CUM GAS & CUM WATER VS. TIME

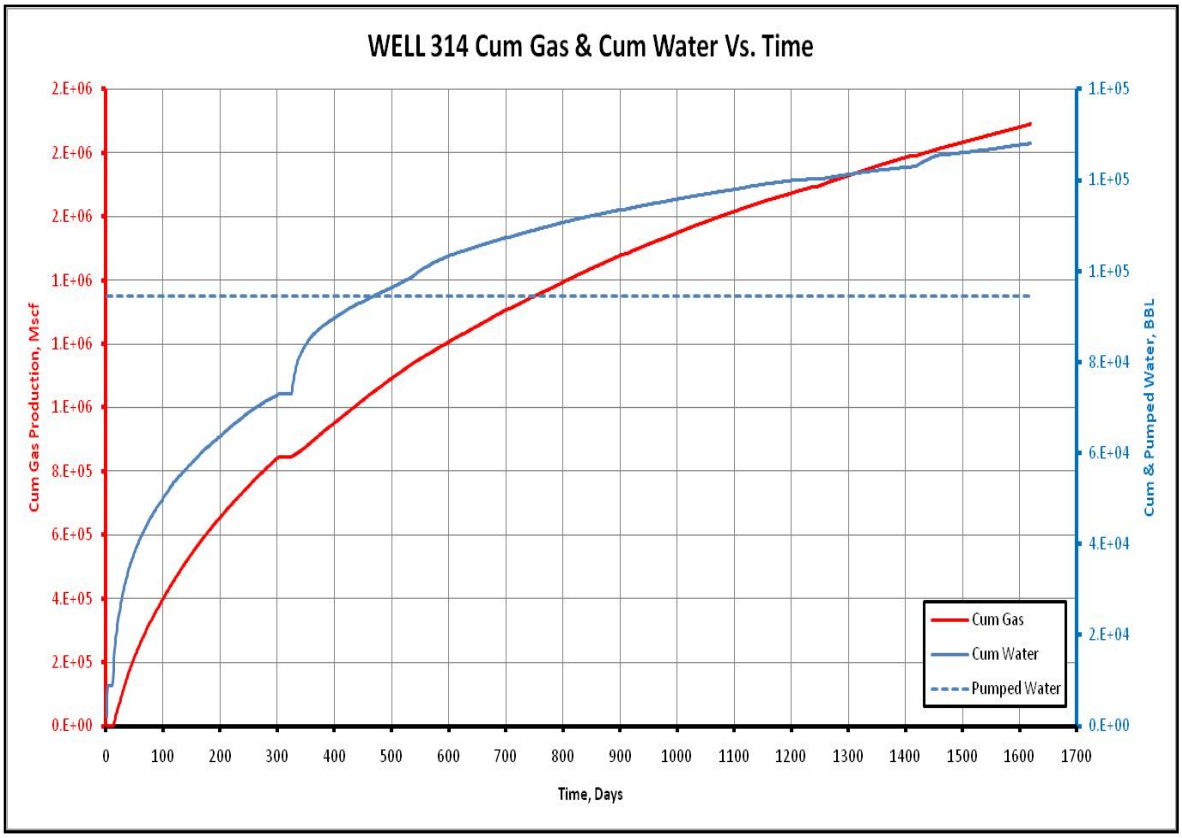

Fig. E-1- Well 314 cumulative gas and cumulative water vs. time. The plot shows that the well produces more water than the injected during hydraulic fracturing which indicates the presence of another water source.

VITA

Name: Hassan Hasan H. Hamam

Permanent Address: Harold Vance Dept. of Petroleum Engineering

TAMU, College Station, TX 77843-3116.

Email Address: Hass1402@yahoo.com

Education: M.Sc., Petroleum Engineering

Texas A&M University

College Station, TX, 2010.

B.Sc., Petroleum Engineering

West Virginia University

Morgantown, WV, 2005.